Chapter 8
The Arc–Continent Collision in Taiwan

T. Byrne, Y.-C. Chan, R.-J. Rau, C.-Y. Lu, Y.-H. Lee, and Y.-J. Wang

8.1 Introduction

Geologists have long been fascinated with the map view curvature of mountain belts (Chamberlain and Shepard 1923; Dana 1866) and one of the many challenges has been to relate orogenic curvature to orogenic processes. Marshak (2004) presents a modern summary and overview of map-view curves and proposes fundamental differences between fold-and-thrust belts that form in pre-deformational basins and belts that form adjacent to obstacles or promontories. The former often form salients whereas the later form recesses or syntaxes in the orogenic belt. Macedo and Marshak (1999) examined the structural consequence of irregularities in the footwall in more detail and pointed out the in the majority of cases, fold and thrust belts tend to advance over pre-deformational sedimentary basins. Thomas (2006) also recently reviewed the importance of structural inheritance in the formation of the Appalachian orogenic belt and reached a similar conclusion – map view curvature often mimics irregularities in the initial continental margin.

In this chapter, we examine the tectonic setting and geologic history of the arc–continent collision in Taiwan, looking in particular at the role of continental margin geometry in the subducting passive margin of the South China Sea. A previously recognized magnetic anomaly along the northern margin of the South China Sea serves as a proxy for the edge of continental crust of normal thickness (~30 km) in this area and can be traced into the central part of Taiwan. The magmatic arc south of Taiwan also appears to record the progressive subduction of oceanic, transitional and continental crust from south to north, defining pre-, early and late collision zones, respectively. One of our objectives is to examine the arc–continental collision, exposed primarily on the island of Taiwan, in the context of this progressive evolution from pre- to late-stage collision. We propose that the continental crust involved in the late stage of the collision is of normal thickness but highly irregular in map view. Based on a combination of magnetic, seismic, geodetic, and topographic data we propose that a continental margin promontory and associated transform fault played, and continues to play, a critical role in the development of the active arc–continent collision in Taiwan.

8.2 Tectonic Setting and Regional-Scale Orogenic Processes

The Taiwan orogenic system is the result of collision of the Luzon arc with the Asian continental margin as

T. Byrne
Center for Integrative Geosciences, University of Connecticut, Storrs, CT, USA
e-mail: timothybyrne@earthlink.net

Y.-C. Chan
Institute of Earth Sciences, Academia Sinica, Taipei, Taiwan, ROC

R.-J. Rau
Department of Earth Sciences, National Cheng Kung University, Tainan, Taiwan, ROC

C.-Y. Lu
Department of Geological Sciences, National Taiwan University, Taipei, Taiwan, ROC

Y.-H. Lee
Earth and Environmental Sciences, National Chung Cheng University, Chiayi, Taiwan, ROC

Y.-J. Wang
Institute of Geophysics, National Central University, Jhungli, Taiwan, ROC

D. Brown and P.D. Ryan (eds.), *Arc-Continent Collision*, Frontiers in Earth Sciences,
DOI 10.1007/978-3-540-88558-0_8,

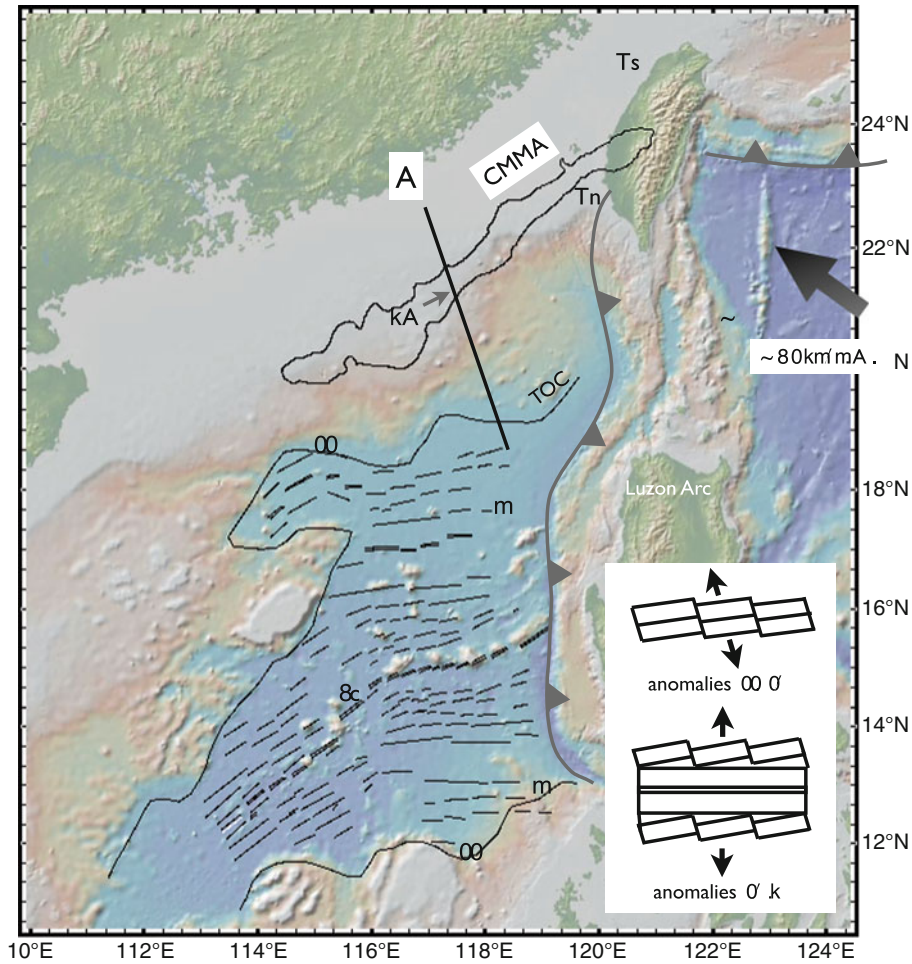

Fig. 8.1 Regional map of South China Sea showing ocean floor magnetic anomalies (from Briais et al. 1989) and continental margin magnetic anomaly (CMMA) from (Hsu et al. 1998). Ts = Taishi Basin; Tn = Tainan Basin; TOC = transitional-ocean crust boundary; black numbers = magnetic anomaly numbers; A = cross-section line in Fig. 8.3; "B" locates Batan Island and *arrow* locates shot-point station 7A in Fig. 8.3. Note westward retreat of Luzon arc over oceanic crust. In this and subsequent figures large *black arrow* shows relative motion vector od Philippine Sea plate with respect to Eurasia. Base map is from GeoMapApp (http://www.geomapap.org) using topography from Ryan et al. (2009).

the South China Sea closes by east-dipping subduction (Fig. 8.1). In the vicinity of Taiwan, the NUVEL-1 global plate motion model predicts that the Philippine Sea plate moves to the NW (~305°–310°) at a rate of 70 km/Ma relative to the Eurasian plate (Seno et al. 1993). Recent GPS data support a similar orientation (~305°–310°) with a slightly larger magnitude (82 km/Ma) (Yu et al. 1997). This relative plate motion vector is 15°–20° clockwise with respect to the orthogonal to the mountain belt; that is, convergence is slightly oblique in the collision zone.

In addition, the obliquity between the north-trending Luzon volcanic arc and the northeast-trending Asian passive continental margin suggests a time-for-space equivalence, thereby providing an opportunity to study the progression from subduction to collision (Fig. 8.2). That is, different positions along the mountain belt may be viewed as different time slices across the collision. Based on the current geometries of the arc and continental margin and current plate kinematics, the collision appears to be propagating southward at a rate of approximately 60 km/Ma (Byrne and Liu 2002b). However, this rate may have varied through time as the geometry of the colliding boundaries and relative plate motions may have changed over time. Suppe (1981) was the first to take advantage of the

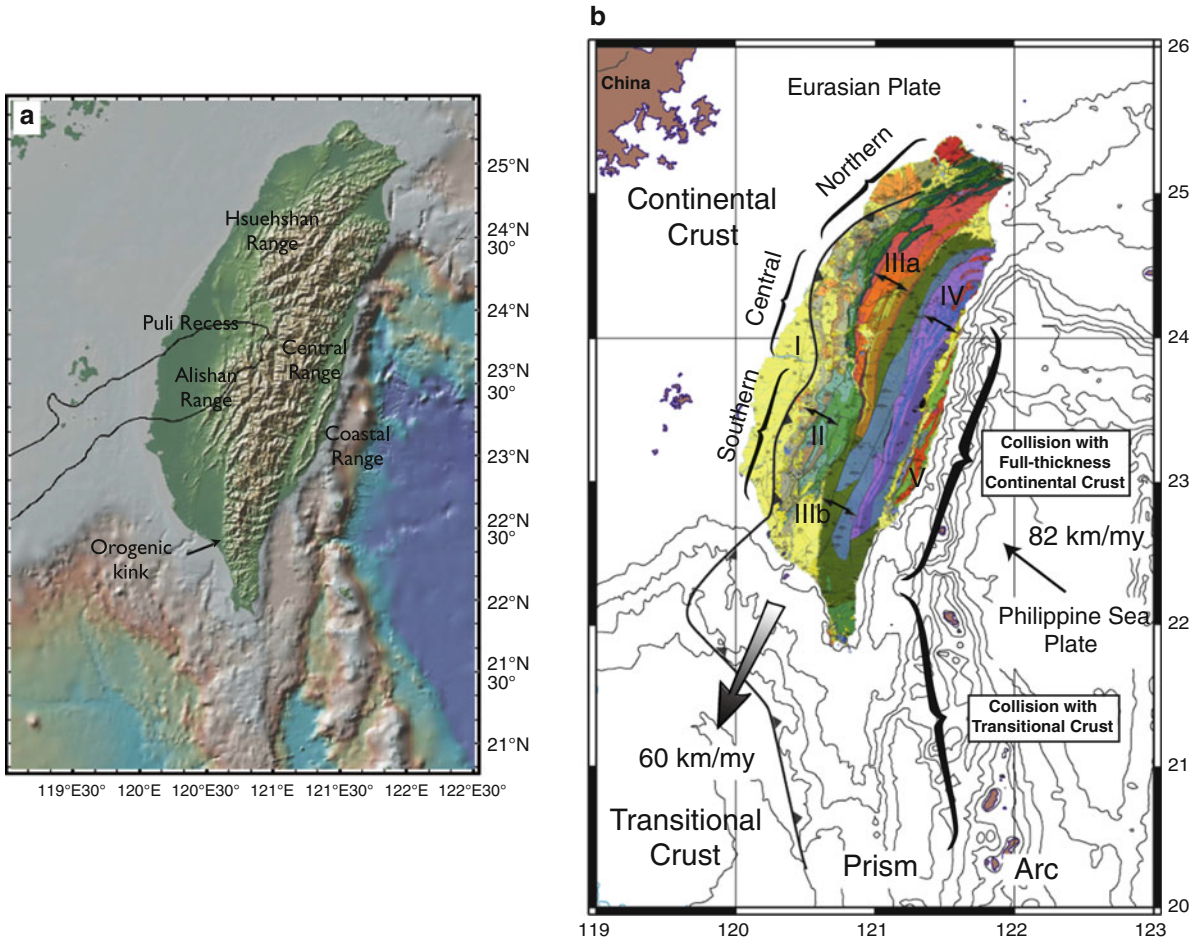

Fig. 8.2 (**a**) Topographic and (**b**) geologic (Chen 2000) maps of Taiwan. I – Coastal Plain; II – fold-and-thrust belt; IIIa and IIIb – slate belts; IV – pre-Tertiary metamorphic belt; V – Coastal Range. *Small arrow*: plate convergence vector, *large arrow*: propagation direction based on plate kinematics (Byrne and Liu 2002b). Note "kink" in southern Taiwan boundary between early and late collision. *Thin black line* in (A) shows outline of CMMA in Fig. 8.1. Base map is from GeoMapApp in (**a**) (http://www.geomapap.org) using topography from Ryan et al. (2009).

space-time equivalence in Taiwan and proposed an evolutionary scenario for the orogen. Assuming a steadily propagating collision and observations of a relatively uniform wedge width, cross-sectional area, and topographic slope, Suppe (1981), building on earlier work by Chapple (1978), inferred that both the size and shape of Taiwan were steady over million-year time scales. Dahlen et al. (1984) and Davis et al. (1983) incorporated this concept of a steady size and shape and proposed the critical wedge theory for steady-state orogens. The key assumption behind the steady-state model is that stresses within the wedge and along the basal décollement are at the Coulomb yield stress. As a result, a critical wedge maintains a constant taper angle (topographic slope + basal slope), which is a function of the décollement dip and the mechanical strengths of the wedge interior and base. Davis et al. (1983) interpreted the relative uniformity of the topographic slope of western Taiwan as evidence of a steady taper angle and, hence, steady crustal strength over the duration of the collision.

Though steady propagation continues to be a fundamental assumption underpinning many recent studies of Taiwan (e.g., Fuller et al. 2006; Stolar et al. 2007b; Willett et al. 2003), there is ongoing debate about whether collision propagation is instead punctuated (e.g., Lee et al. 2006; Mouthereau et al. 2002; Mouthereau and Lacombe 2006) or much slower than previously expected (e.g., Simoes et al. 2007). Indeed, one of the first detailed studies of geomorphic

parameters in the eastern Central Range (Willemin and Knuepfer 1994) indicated higher uplift rates in the central part of the range rather than in the south as predicted by the propagation interpretation. Recent research along the western Central Range also suggests higher uplift rates in the middle of the range (Byrne et al. 2009). These results are consistent with completely reset fission track ages of detrital zircons from southern Taiwan that show exhumation ages substantially older than predicted by southward propagation (e.g., 6 Ma vs. <1 Ma., Lee et al. 2006). In contrast to these results, Ramsay et al. (2007) have recently shown that the geomorphic patterns and indices in the southern most part of the Central Range are consistent with southward propagation, although the age and rates are not well constrained.

Several alternative models of the orogen have been proposed since the original critical wedge interpretations (Davis et al. 1983; Dahlen et al. 1984; Dahlen and Barr 1989). These early models, rather than treating the Central Range as a rigid backstop, have attempted to explain both the regional-scale topography and vergence of deformation of the Taiwan orogen. One of the first alternative models proposed that the orogen is a doubly vergent critical wedge (Koons 1990; Willett et al. 1993) consisting of a shallow-tapered western wedge, which extends from the toe of the fold-and-thrust belt to the main topographic divide, and a more steeply-tapered eastern wedge, which extends from the divide to the eastern edge of the Central Range (e.g., Willett et al. 2003; Whipple and Meade 2004, 2006).

A second model, presented by Carena et al. (2002), proposes that the Taiwan orogen, from the fold-and-thrust belt to the eastern Central Range, is a single west-vergent critical wedge. The rollover in topography at the main divide is explained by roll-over of the basal decollément (i.e., maintenance of a constant taper requires an eastward-dipping topographic slope). The backstop in this model, though not explicitly specified by Carena et al. (2002), is presumably the Luzon Arc and Coastal Range onshore.

Simoes et al. (2007) proposed a third model, which departs from critical wedge theory, that holds that the main components of the Taiwan orogen (e.g., the Hsüehshan, Backbone, and Central Ranges) act as rigid blocks and slide past each other along high-angle reverse faults (Simoes et al. 2007). In this model, the wedge is bounded to the east by a steeply dipping normal fault that raises the eastern Central Range over the Longitudinal Valley; the geometry and sense of slip along this fault are required to explain high maximum temperatures achieved by material inferred to be underplated beneath the Central Range. Because the physical basis for underplating is not known with certainty, the spatial patterns of mass influx and efflux are not necessarily related in the model of Simoes et al. (2007), and therefore, there is a wider range of allowable responses to surface erosion than in the critical wedge model.

Finally, Yamato et al. (2009) present a fully coupled thermomechanical numerical model that is consistent with much of the geological and geophysical data from Taiwan. Similar to a limited number of earlier studies (Wu et al. 1997; Lin 2000; Lin et al. 1998), Yamato et al. (2009) conclude that the orogen is "thick-skinned". In this context, they propose that deep-seated materials from the Chinese crust drive exhumation and erosion of the Central Range. In contrast to previous studies (e.g., Simoes et al. 2007), however, Yamato et al. (2009) propose that exhumation is related to frontal accretion of the whole (bi-layered, in their model) Asian continental crust. Their results also imply that the eastward increase in metamorphic grade across the orogen is related to the initial depth of the rocks, rather than significant subduction.

Investigations of the age of collision initiation have also been inconclusive. A relatively rapid increase in rates of deposition (Chen et al. 2001) and the age of the oldest sediments derived from the orogen (Lundberg and Dorsey 1990; Huang et al. 2006) suggest the collision initiated 3–4 Ma (Suppe 1984). Paleomagnetic data also show that collision-related clockwise rotation of the arc in the Coastal Range started about 2–3 Ma. These ages, however, may be minimum estimates because the northern part of the arc appears to be partially subducted beneath northern Taiwan and the Ryukyu arc. Older ages for collision initiation (~ 6 Ma) come from age of basin subsidence in the foreland, interpreted to be related to orogenic loading (Lin et al. 2003; Lin and Watts 2002; Simoes and Avouac 2006), and from fission track ages of completely reset detrital zircons from the Central Range (Liu et al. 2000, 2001; Lee et al. 2006). Lee et al. (2006) have recently proposed that both suites of ages may be correct and that the collision progressed in stages.

In northern Taiwan, the polarity of subduction is reversed and the volcanic rocks of the Luzon arc and the oceanic crust of the Philippine Sea plate are subducting to the northeast along the Ryuku trench (Suppe 1984; Yu et al. 1997; Wu et al. 2009). Subduction of the

Philippine Sea plate is evidenced by patterns of deep seismicity coinciding with high P-wave velocities (Wu et al. 2009; Rau and Wu 1995; Chou et al. 2009). Subduction in this area has also resulted in westward propagation of the Okinawa Trough into northeastern Taiwan, generating extension and orogenic collapse (Teng 1996). These data support the interpretation that the Taiwan orogenic system exhibits the full range of tectonic behavior from pre-collision in the southern offshore region, to active collision in southern and central Taiwan, to post-collision in northern Taiwan.

8.3 Geologic Background

Within the collision zone, continental shelf, slope, and rise sediments of the passive margin and part of the underlying basement have been deformed, metamorphosed and accreted (Byrne and Liu 2002a; Ho 1975, 1982; Suppe 1984), forming three tectonostratigraphic units that parallel the topographic grain of the island (Fig. 8.2). The units increase in metamorphic grade and deformational complexity from west to east, forming an active fold-and-thrust belt of Miocene to Quaternary sediments, a slate belt of Eocene to Miocene sediments, and a belt of pre-Tertiary metamorphic rocks. The boundaries between the units appear to be major fault zones, although none of the boundaries appears to be seismically active. All three belts are recognized along the length of the orogen; however, there are significant differences along strike, particularly north and south of the recess, or embayment, of the topographic centered on the city of Puli (Fig. 8.2).

The fold-and-thrust belt appears to display the most variation along strike, particularly around the Puli recess (Fig. 8.2a). North of this recess, a relatively thick, Miocene and younger sedimentary section (up to 8 km) is deformed into a series of tight, north to northeast-trending regional-scale folds with up to 7–8 km of structural relief (e.g., the Chuhuangkeng anticline, Ho 1976; Hung and Wiltschko 1993; Lacombe et al. 2001; Mouthereau et al. 2002; Namson 1981). In the area of the Puli recess in central Taiwan, imbricate sheets of Miocene to Quaternary sedimentary rocks characterize the fold-and-thrust belt, consistent with classic fold-and-thrust belts (e.g., Yue et al. 2005). The north-trending Chelungpu thrust, which generated vertical coseismic displacements of up to 10 m in the 1999 M 7.6 Chi-Chi earthquake, crops out in the middle of this section of the fold-and-thrust belt. The southern section of the fold-and-thrust belt (i.e., south of the recess) is wider than the belt to the north and balanced cross-sections and limited seismic reflection data suggest that it is characterized by duplex structures and/or basement (pre-Miocene)-involved imbricate thrusting (Ho 1976, 1988; Hung and Wiltschko 1993; Mouthereau et al. 2002). Thus, the thrust belt shows large variations in structural style from north to south, with regions in northern Taiwan where a thick sedimentary section is deformed, a central region where the stratigraphic section is thinner and a more classic thrust belt is present, and a southern region where the décollement appears to cut deeper in to the pre-Miocene (i.e., "basement").

The slate belt comprises two sub-belts generally west and east of the Lishan fault (Units IIIa and IIIb in Fig. 8.2b). The western sub-belt is exposed primarily in the Hsüehshan Range although it also continues southward across the Puli recess, where the bedrock is often laterized (Hsieh, M.-L. 2008, personal communication) and continues into the western edge of the Central Range where the sub-belt pinches out. In the Hsüehshan Range an east-dipping cleavage on the west side of the range and a west-dipping cleavage on the east side form a regional-scale popup structure (Clark et al. 1993). In contrast, the eastern sub-belt of the slate belt crops out in the Central Range where it displays a well developed, southeast-dipping structural fabric (Fisher et al. 2002, 2007). Incremental strain markers show a top-to-the-northwest sense of shear (Fisher et al. 2002) throughout the slate belt in this range. Southeast of the Puli recess, the eastern sub-belt supports the highest peak in the orogen (Yushan 3,952 m) and exposes the oldest sediments of the pre-collisional passive margin (the Eocene Shihpachungchi Formation). In the southern Central Range, the slaty cleavage is less penetrative and pencil cleavages are locally present. Further south, in the Hengchun Peninsula, penetrative cleavages are rare to non-existent. These observations show strong along- and across-strike structural variability internal to the slate belt.

The Tananao schist, a complex of multiply deformed metasediment, marble, and granite in the eastern Central Range, is interpreted as exhumed Eurasian continental basement (Ho 1986). Regionally, the Tananao schist has been subdivided into two belts: (1) the High T/Low P Tailuko belt (of Taroko gorge) and (2) the High P/Low T greenstones and schists of the Yuli belt.

Together, these belts are interpreted to represent the remnants of a late Mesozoic subduction complex that was thinned during Tertiary rifting prior to being incorporated into the Taiwan orogenic wedge (Yui et al. 1990). The interpretation of fabrics and paleotemperatures in the Tananao schist, however, is hampered by the difficulty in differentiating Mesozoic deformation and metamorphism from features related to the ongoing collision.

The Longitudinal Valley, a relatively straight basin that separates the Asian basement and cover of the Central Range from the accreted arc complex of the Coastal Range represents one of the most enigmatic morphotectonic features in Taiwan. The mountain fronts that define the western and eastern margins of the valley are in places demonstrably active (e.g., Lee et al. 2001, 2002) or recently active (e.g., Shyu et al. 2006) fault zones with shortening rates on individual faults locally as high as 15 mm per year (Angelier et al. 1997; Lee et al. 2002). Moreover, leveling surveys across the southern part of the valley indicate uplift of both the Central and Coastal Ranges relative to the valley floor at a rate of ~3 cm per year (Liu and Yu 1990). Thus, the flanks of the Longitudinal Valley are everywhere a site of rapid horizontal and vertical deformation, yet this feature persists along the length of the active collision zone.

The Coastal Range of easternmost Taiwan represents the northern extension of the Luzon volcanic arc and forearc basin that has collided with and accreted to Taiwan. The arc complex consists of a lower Miocene sequence of intermediate to mafic volcanic and shallow intrusive rocks, a middle to upper Miocene sequence of marine pyroclastics, andesitic tuff, lapilli tuff and tuff breccia, and finally, an arc-fringing carbonate reef complex (Ho 1986). The arc complex is unconformably overlain by a 4–6.5-km-thick collisional Plio-Pleistocene basin sequence derived from the Central Range to the west (Dorsey 1992). This syncollisional sequence records rapid subsidence of the arc complex and unroofing of the mountain belt to the west, with increasing metamorphic grade of lithic fragments up section (Dorsey 1992). A series of Holocene elevated shorelines along the east coast of the Coastal Range indicates active uplift, with rapid uplift rates of ~2.5 to >8 mm per year (Liew et al. 1993). However, recent compilations of continuous GPS in the northern Coastal Range (Lin et al. 2010) show significant subsidence relative to the Longitudinal Valley and the Central Range. These results are consistent with interpretations of seismicity and Vp tomography indicating subduction of the arc beneath the Ryukyu subduction zone.

8.4 The Chinese Passive Margin: The Collisional Footwall

The South China Sea is a relatively large marginal basin of mid-Tertiary age surrounded on three sides by blocks of continental crust (Fig. 8.1). The middle of the basin is composed of oceanic crust and preserves several sets of magnetic anomalies (Hayes and Taylor 1978). The northern and southern margins are passive margins that formed as the basin opened whereas the western boundary appears to be a left-lateral transfer zone that may connect to the Red River fault in China. In fact, Briais et al. (1993) have argued that the basin formed in conjuncture with large (500–600 km) left-lateral displacements along the Red River fault as India collided with Eurasia. Briais et al. (1993) also completed a detailed study of the anomalies in the middle of the basin and proposed a complicated spreading history that included asymmetric spreading, propagating ridges and ridge jumps. In general, however, the history is marked by three directions of spreading (Fig. 8.1 inset): an initial phase of NW–SE spreading (32–30 Ma; anomalies 11 and 10), a middle phase of N–S spreading (30–24 Ma; anomalies 10–6b) and a late phase of NW–SE spreading (24–18 Ma; anomalies 6b to 5a). The earliest phase of NW–SE spreading appears to have defined the generally geometry of the continental margins, including the area of the arc–continent collision in Taiwan.

Nissen et al. (1995) investigated the structure and general composition of the margin of the South China Sea south of the collision and documented a relatively wide zone of transitional crust (~250 km across strike, Fig. 8.3) composed of thinned continental crust, volcanic and other igneous rocks, and a high velocity lower crust. Nissen et al. (1995) interpreted the high velocity lower crust as underplated gabbroic rocks and proposed that the steep boundary between these rocks and more continental-like rocks in the lower crust to the north was responsible for a magnetic anomaly observed at the surface. Wang et al. (2006) recently confirmed this transition in the lower crust

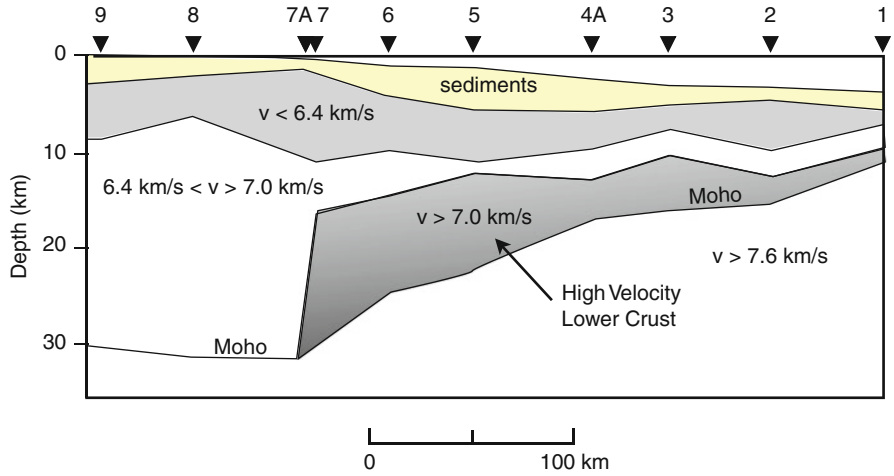

Fig. 8.3 Geophysical cross-section from Nissen et al. (1995). Numbers show range of velocities (km/s) in crustal layers. Note dramatic thinning of continental crust from a normal thickness of ~30 to ~5 km from at shot-point 7A. Dark shaded layer below thinned crust (labeled) is interpreted by Nissen et al. (1995) to be gabbroic in composition.

using higher resolution data from ocean bottom seismometers. The magnetic map of this region shows a northeast trending linear high that lies just landward of the continental shelf (Fig. 8.1) (Wang et al. 2002; Hsu et al. 1998), consistent with Nissen's (1995) interpretation that it can be used as a proxy for the boundary between continental and transitional crust.

The magnetic high also continues into central Taiwan where it is parallel to the seaward edge of a previously recognized basement high (Fig. 8.4) (i.e., Peikang High; see also Cheng 2004 for a similar interpretation). The magnetic high (Fig. 8.4a), however, extends further northeast into central Taiwan and appears to be truncated or offset long a northwest-trending fault or fracture zone (Fig. 8.4a). The apparent fracture zone is parallel to the early spreading direction in the South China Sea (i.e., NW–SE, Fig. 8.1) and orthogonal to the trend of pre-breakup (~58–30 Ma) sedimentary basin (e.g., the Nanjihtao Basin, Lin et al. 2003) along the margin. We therefore propose that the northwest trending truncation of the magnetic anomaly represents a partially subducted continental margin fracture zone in the passive margin of Eurasia.

Seismic reflection data and subsidence records of deep wells provide additional constraints on the evolution of the margin in the area of Taiwan and show two en echelon, post-rift sedimentary basins, centered on the magnetic anomaly (Fig. 8.4b). The northern, or Taishi, basin, records deposition throughout the Eocene, Oligocene and Miocene and is preserved both offshore northwestern Taiwan (Lin et al. 2003; Teng 1987) and in the sedimentary record of the Hsüehshan Range (Teng 1987). The southern, or Tainan, basin records deposition of Miocene sediments and is preserved offshore southwest of Taiwan; an earlier record of Eocene to Oligocene deposition may have been removed by late Oligocene uplift and erosion in this area (Lin et al. 2003). The eastern slate belt in the southern Central Range, which is also missing an Oligocene section, may be the exhumed equivalent of the Tainan Basin. The slate belt, however, also exposes Eocene sediments, suggesting that both sedimentary basins may have contained Eocene sediments.

The magnetic anomaly between the two en echelon basins widens slightly and the anomaly's seaward edge curves from 60° to 75°, consistent with the recognized reorientation of the spreading direction in the South China Sea at the time of anomaly 10 (~30 Ma) (Fig. 8.1 inset). Normal faults that bound the Tainan Basin south of the anomaly are also slightly curved. North of the anomaly, the western edge the Taishi Basin (30–6.5 Ma) (Fig. 8.4b) occupies the triangular zone between the anomaly and the fracture zone (Fig. 8.4), suggesting that the basin propagated across the fracture zone as the spreading direction changed and the magnetic anomaly rotated seaward. This slight reorientation and extension north of the anomaly may have also isolated a fragment of continental crust, forming the Peikang High.

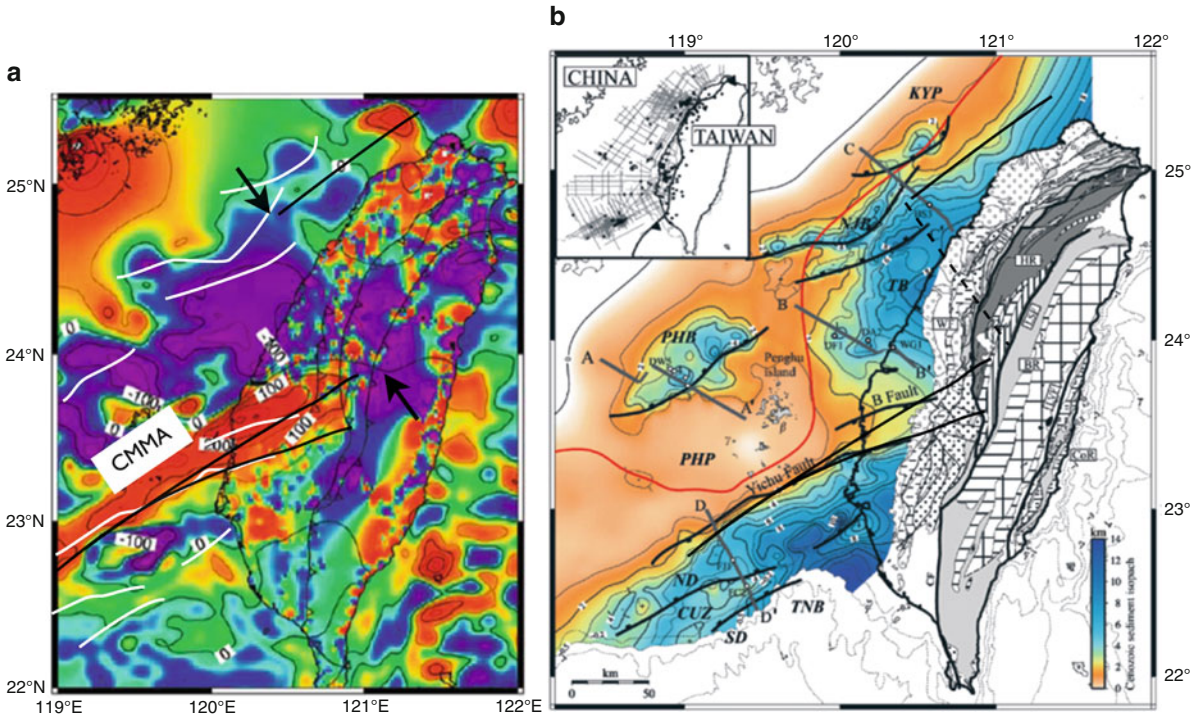

Fig. 8.4 (**a**) Magnetic anomaly (Cheng 2004) and (**b**) depth to Mesozoic basement (Lin et al. 2003) maps. *Arrows* in (**a**) show trend and extent of interpreted fracture zone that truncates magnetic anomaly. *Dashed black line* in (**b**) shows Interpreted fracture zone. *Straight black lines* show interpreted edge of continental crust based on magnetic anomaly and Mesozoic basement morphology; these lines are shown in subsequent figures for reference. *White lines* in (**a**) are normal faults shown as *black lines* in (**b**). Contours in (**a**) are nanoteslas. CUZ = Central Uplift Zone; KYP = Kuanyin Platform; ND = Northern Depression; NJB = Nanjihtao Basin; PHB = Penghu Basin; PHP = Penghu Platform (or high); SD = Southern-Depression,TNB = Tainan Basin,TB5 = Taihsi Basin; BR = Backbone Range; CoR = Coastal Range; HR = Hsüehshan Range; WF = Western Foothills. Major faults: CF = Chaochou; CHF = Chuchih, LSF = Lishan; LVF = Longitudinal Valley.

The western edge of the Taishi Basin, which crosses the proposed fracture zone and laps onto the Peikang High, preserves a progressively thicker Miocene section from southwest to northeast (Fig. 8.4b). For example, near the Peikang High the Miocene is only a few hundred meters thick whereas northeast of the fracture zone it is 2–3 km thick. The rates of deposition during the Miocene also increase to the northeast from 35 m/Ma near the Peikang High to 120–190 m/Ma north of the fracture zone (Lin et al. 2003; Mouthereau et al. 2002). Although this change in deposition may be gradational, previous authors have proposed that it may also occur in two northwest-trending steps, one near the Peikang High (recognized as the Pakushan transfer zone) (Deffontaines et al. 1994; Mouthereau et al. 2002) and the second parallel to the proposed fracture zone (recognized as the Sanyi-Puli transfer zone) (Lee et al. 1997; Rau and Wu 1995; Deffontaines et al. 1994, 1997).

In summary, rifting in the South China Sea appears to have formed a relatively wide area of transitional crust, including a continental margin magnetic anomaly (CMMA). Based on geophysical data along the margin in the South China Sea, the CMMA serves as a proxy for the edge of a continental crust of normal thickness (~30 km). In Taiwan, the anomaly appears to be truncated by a northwest-trending fracture zone, defining a continental margin prong or promontory. Two post-rift sedimentary basins formed "en echelon" north and south of the truncated anomaly and the northern basin appears to have propagated across the fracture zone during a change in spreading direction. In the following sections we evaluate the role that the wide zone of transitional crust and the continental promontory, including its sedimentary cover, played in the collision. For easy reference, the black lines (continuous and dashed) in Fig. 8.4 are used in subsequent figures to represent the seaward edge of the continental margin.

8.5 Luzon Magmatic Arc: The Collisional Hanging Wall

The Luzon arc records subduction-related volcanism since at least the early Miocene (16–15 Ma) (Yang et al. 1995, 1996) and provides important clues to the evolution of the collision as the subducting plate changes from oceanic to continental crust. Although the arc is generally typical of subduction zone magmatic arcs and broadly andesitic in composition, several regional-scale segments have been recognized along strike. For example, the segments north and south of Luzon Island appear to have been pinned, or slowed, by thicker crust in the subducting plate (Fig. 8.1). In the north, the "S-shaped" inflection in the deformation front (Fig. 8.1) correlates with the boundary between oceanic crust in the south to transitional crust in the north whereas in the south, collision of the Palawan Ridge appears to be limiting westward migration of the arc. As a result, the central segment (Luzon) has retreated westward over the oceanic crust of the South China Sea. Similar arc geometries above oceanic lithosphere with changing physical properties along strike have been documented at a number of margins around the world (Wallace et al. 2005; Vogt et al. 1976; McCabe 1984), consistent with the observations from Luzon.

The northern segment (e.g., north of Luzon) also appears to be segmented. Well-developed, stratavolcanoes of Quaternary age occur in northern Luzon Island and as far north as Batan Island (20.5°N, Fig. 8.1), about 100 km south of Taiwan. Relatively young K–Ar ages (30 ka) have also been reported from the islands just south of Taiwan, but volcanic activity this far north appears to be more limited. The volcanic rocks in the area of Batan Island are also distinctive in containing mantle xenoliths and geochemical signatures that suggest the involvement of enriched mantle considered to reside in the continental lithosphere (Yang et al. 1995, 1996). Yang et al. (1996) has also recognized a double arc, with older arc rocks to the west, south of Batan but not north of it. Yang et al. (1996) has also pointed out that this unusual along-strike change in arc character and composition correlates with a relatively abrupt change in the dip of the slab from shallow in the south to nearly vertical in the north, possibly resulting in a tear in the slab in this area and allowing lateral flow of Eurasian mantle. Yang et al. (1996) suggested that the partial subduction of the inactive South China Sea spreading center beneath Luzon resulted in shallowing of the subduction zone, leading lateral flow of the mantle and arc contamination.

Alternatively, the area of the proposed broken slab (approximately Batan Island) also correlates with the transition from oceanic to transitional crust in the subducting plate. We, therefore, propose that westward retreat of the central segment of the Luzon arc over oceanic crust caused shallowing of the slab in this area, leading to the tear proposed by Yang et al. (1996). In this interpretation, the pinning of the arc north of Luzon by the subduction of transitional crust marks the initial stages of the arc–continent collision in Taiwan. This initial collision, however, is between the arc and transitional crust rather than between the arc and continental crust of normal thickness.

Collision of transitional crust with the arc also appears to be recorded in the geology and morphology of the arc and forearc north of Batan Island. At about 21°N lat. (about 50 km north of Batan, Fig. 8.1) the accretionary prism associated with the Manilla Trench widens from about 30 km to nearly 60 km, consistent with subduction thicker crust and/or the influx of offscraped or underplated materials into the wedge. Slightly further north (~ 21.25°N) a well-defined back thrust (i.e., a west-dipping thrust) in the Luzon forearc signals the collapse of the forearc (Malavieille and Trullenque 2009), indicating that the colliding materials are of sufficient strength to transmit horizontal stresses within the forearc. Detailed structural studies of the forearc in this area also show that the back thrust overlies a more significant, east-dipping thrust that separates the underthrusted forearc from relatively undeformed arc. Cheng (2008), based on P-wave tomography has also proposed that the relatively thin crust of the forearc is progressively thrust beneath the arc from about 21°N to 23°N where it appears to lie completely beneath the arc.

Paleomagnetic studies of the arc rocks in the Coastal Range of Taiwan provide additional information about the kinematics and timing of the collision. Lee et al. (1991) collected sedimentary samples from 132 sites that overlie the arc volcanic rocks and range in age from early Pliocene to Pleistocene. Based on the age and paleomagnetic characteristics of each site, Lee et al. (1991) divided the range into northern, central and southern sections. He also recognized an older and a younger suite of sites in each section. The results

show that all three geographic sections record 20° to 25° of clockwise rotation, and that the rotations are diachronous from north to south. In the north, rotation of the arc occurred 2–3 Ma, whereas in the central section it occurred 2.1–1.7 Ma and in the south it occurred after about 1.4 Ma. The data also suggest that the rotations occurred relatively quickly at each site (~0.5 m.y.), and that the rotation migrated southward at about 70 km/Ma. This migration rate is only slightly higher than the most recent calculations for the rate of collision propagation of 60 km/Ma (Byrne and Liu 2002b). A sharp clockwise bend in the topographic grain of the orogen about 70 km south of the Coastal Range (at about 22.3°N lat) is also consistent with this propagation rate and suggests that the bend in the topographic grain marks the area of active, collision-related oroclinal bending.

Finally, isotopic and geochronologic data from accreted volcanic centers in the Coastal Range show a systematic trend in geochemical signatures and in the age of youngest volcanism. In the north, the top of the volcanic rocks yield dates of NN11 (< 8–5 Ma, Chi et al. 1981) and 6–5 Ma (40Ar/39Ar; Lo and Onstott 1995) whereas the top of the same stratigraphic horizon in the south yields ages of 5.6 Ma (40Ar/39Ar; Lo and Onstott 1995). Volcanism in the offshore Lutao and Lanhsu Islands ended at 1.5 Ma and 0.5–0.04 Ma (Yang et al. 1995), respectively. Thus, both the microfossil and radiometric ages indicate that the initial arc–continent collision began at ca. 6–5 Ma in the north and propagated southward. A progressive increase in continental contamination of magmas also correlates with progressively younger ages the volcanic rocks and is interpreted to reflect the systematic increase in continentally derived sediments through time (Dorsey 1992).

In summary, the arc south of Taiwan records significant changes in its structure, age and chemical signature hundreds of kilometers before it collides with the continental margin of China in the area of Taiwan. These along-strike changes appear to reflect the subduction of a relatively wide zone of transitional crust rather than well-developed oceanic crust. We propose therefore that the "early collision zone" extends from Batan Island (i.e., approximate boundary of oceanic to transitional crust in the subduction plate) to the zone of active oroclinal bending (i.e., the kink in topography) in southern Taiwan. This is an along-strike distance of about 200 km, which, assuming a collision propagation rate of 60 km/m.y., suggests that the initial collision (of transitional crust) may have started nearly 3 Ma before the arc collided with continental crust of normal thickness. In addition, because the trend of the boundary between transitional and oceanic crust strikes more easterly than the strike of the continental margin, the propagation rate of the collision with transitional crust would have been slower by about a third. The collision (initially with transitional crust), therefore, may have started 6–7 Ma.

8.6 The Collision Zone: Implications of Transitional Crust and a Continental Margin Promontory in Collision Kinematics, Dynamics and Exhumation

Here we examine the arc–continent collision in Taiwan in more detail and evaluate the role that subducting crust of variable composition and thickness may have played, and may continue to play, in the development of the orogenic system. In the previous sections we proposed that the boundary between oceanic and transitional crust marks the transition from normal subduction, south of the boundary, to collision north of the boundary. That is, the subduction-collision transition occurs about 200 km of Taiwan, near Batan Island. This location of the transition is significantly farther south than most previous interpretation that place the transition closer to Taiwan (Huang et al. 2006; Suppe 1984; Malavieille and Trullenque 2009). Teng (1990) is a notable exception as he also recognized the wide zone of transitional crust and proposed that the collision may have started 6–8 Ma. Based on the clear correlation between changes in the subducting plate and the growth of the prism and the collapse of the forearc to the north, we propose a two-staged collision: An early stage of the collision from Batan (i.e., ~ lat 21°N) northward to the "kink" or orocline in the orogenic topography in southern Taiwan (Figs. 8.1 and 8.2) and a late, or current stage of the collision from the kink to northern Taiwan where the Central Range is subsiding on the southern flank of the Okinawa Trough and the arc is subducting beneath the Ryukyu trench.

8.6.1 Early Stage of the Collision

This stage of the collision is primarily preserved in the off shore region south of Taiwan, which is only accessible remotely, and on the Hengchun Peninsula. Available data indicate that as progressively thicker transitional crust is subducted from south to north the depth of the sea floor at the Manila Trench shallows and the composition of the sediments on the subducting plate changes from dominantly hemipelagic clays and silts in the south to silts and sands in the north (Yu and Huang 2009). Seismic reflection data also show that at shallow structural levels near the deformation front the décollement is relatively deep as nearly all of the sediments on the subducting plate are being accreted (Yu and Huang 2009; McIntosh et al. 2005). Thus, at deeper structural levels in the prism, where the décollement probably steps to deeper levels, blocks of transitional crust also may be incorporated into the prism.

Detailed geophysical studies across the early collision in southern Taiwan also show sediment accretion and suggest the possible involvement of crustal rocks. For example, McIntosh et al. (2005) recognized a relatively high P-wave velocity core beneath the Hengchun Peninsula in southern Taiwan with velocities that are consist with either metamorphosed accretionary prism materials or accreted basement from the subducting transitional crust. In addition, Cheng (2008) (Fig. 8.5) has recognized blocks of anomalously high velocity and density further north in the southern Central Range. The blocks were mapped using high-resolution seismic tomography of both Vp and Vs waves integrated with a gravity model. The Vp and Vs waves also provide Poisson's ratio (σ). Cheng (2008) was able to recognize at least 3 km-sized

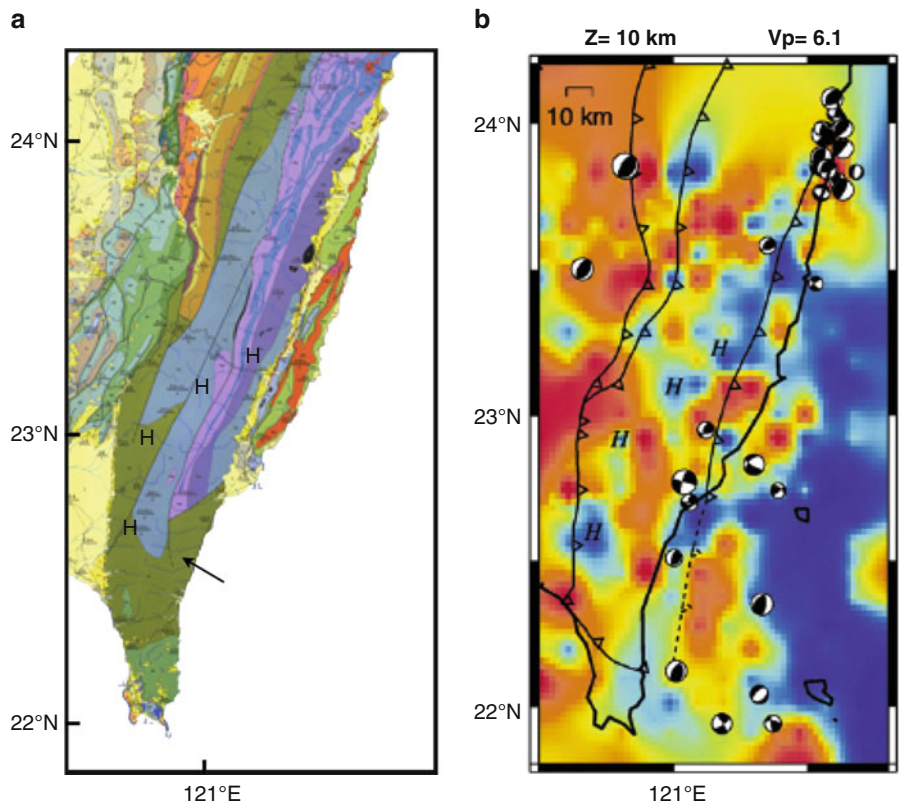

Fig. 8.5 (**a**) Geologic map of the southern Central Range (Chen 2000) and (**b**) map view of Vp velocity structure at 10 km depth (Cheng 2008). "H" shows locations of high velocity anomalies interpreted as accreted blocks of mafic (transitional?) crust. Note strip of mafic rocks in Central Range and locations of anomalously old reset fission track ages [*arrow* in (**a**)](Liu et al. 2001; Lee et al. 2006).

blocks in the upper and middle crust of the Central Range with anomalously high Vp and high σ, which he interpreted as representing slivers of mafic crust. Because the blocks are interpreted to be slivers in the continental materials of the Central Range (i.e., the pre-Tertiary metamorphic rocks and/or slate belt), Cheng (2008) also proposed that the subducted transitional crust was unusually wide.

Additionally, the only exposed tectonic slivers of mafic rocks that are part of the late Tertiary collision crop out in the area of mafic blocks described by Cheng (2008) (Fig. 8.5). The exposed mafic unit occurs along the faulted contact between the slate belt and the pre-Tertiary metamorphic rocks (Chen 2000). The rocks have not been studied in detail or dated, but may represent pieces of accreted oceanic crust or mantle, or part of an underplated gabbroic sequence. In any case, their occurrence is consistent with geophysical data that indicate similar bodies at depth and suggest the involvement of transitional crust in the early stages of the collision. Eroded equivalents of these mafic blocks may also be preserved in the Kenting mélange (Huang et al. 1985), which is exposed on the southwestern tip of the Central Range.

Evidence for an early stage to the collision in Taiwan also comes from unexpectedly old exhumation ages of accreted sediments exposed in the Central Range. For example, Liu et al. (2001) obtained completely reset zircon fission track ages from sandstones in both northern and southern Taiwan. Liu et al. (2001) interpreted the northern ages as evidence that collision started 6 Ma or earlier. This interpretation is also consistent with cooling ages (4–3.6 Ma) Liu (2000) obtained from sandstone boulders eroded from the Central Range and deposited in the northern Coastal Range, and with the age of the earliest foreland basins (~6.5 Ma; Lin et al. 2003; Simoes and Avouac 2006; Teng 1987).

More recently, Lee et al. (2006) have confirmed the older zircon ages in southern Taiwan documented an additional subset of "old" grains and identified a suite of younger ages for completely reset detrital zircon and apatite grains. Based on these new data, Lee et al. (2006) proposed a multiple stage collision that started ~6 Ma in both northern and southern Taiwan (Fig. 8.6). The younger ages and their distribution in southern Taiwan also suggest to Lee et al. (2006) that the area records an increase in exhumation rates starting about 1–3 Ma and that this stage of relatively rapid uplift may be propagating southward into the area of Hengchun Peninsula. This proposed increase in exhumation cooling supports the hypothesis that the collision is composed of early and late stages.

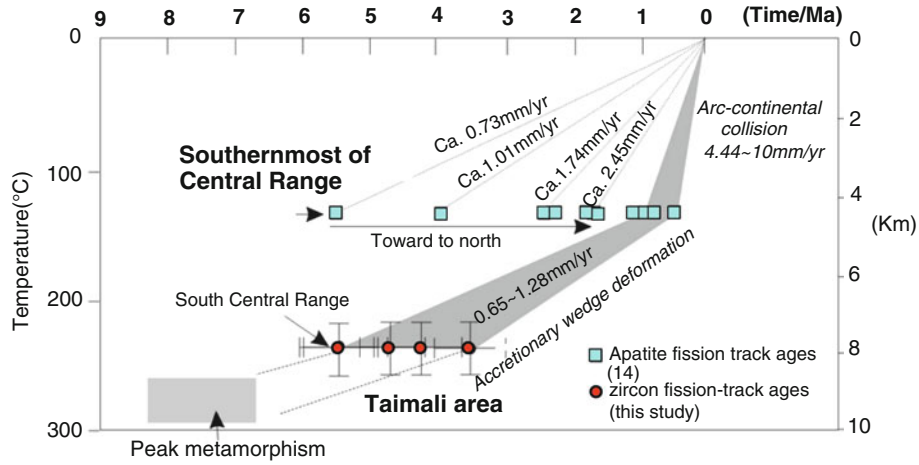

Fig. 8.6 Compilation of completely reset detrital apatite and zircon fission track ages from sandstones in the southern Central Range (from Lee et al. 2006). Data from Taimali area (*shaded*) show a change in exhumation cooling rates from ~1 mm/yr to up to 10 mm/yr at ~1 Ma whereas apatite data from southernmost Central Range show a progressive decrease in ages from south to north. Proposed increase in cooling at ~2 Ma is consistent with the transition from early to late collision stages proposed here.

8.6.2 Late Stage of the Collision

Our discussion of the late stage of the collision progresses from a review of the current state of stress (seismicity) and surface displacements (GPS) to signatures in the topography and structural fabrics and finally to crustal-scale observations and possible evolutionary scenarios of the orogen. Our overall goal is to understand the possible link between the subducting continental margin and the kinematics and dynamics in the early and late stages of the collision. The results strongly suggest: 1) that the continental margin promontory has had significant impact on the evolution of the orogen; 2) that the youngest stage of the collision is fundamentally three-dimensional, and 3) that the southward propagation inferred from the tectonic setting may only apply to the relatively recent history of the Coastal Range and the southern tip of the Central Range.

8.6.2.1 Seismicity

Three well-defined patterns of seismicity in west-central Taiwan appear to reveal the partially subducted continental margin and associated fracture zone. One of the patterns is defined by a steeply dipping, planar cluster of seismicity, generally recognized as the Sanyi-Puli seismic zone (Wu et al. 2004), which parallels the proposed fracture zone (Fig. 8.7a). This zone of activity was particularly well-defined prior to the 1999 Chi-Chi earthquake (Wu et al. 2004) and is composed of an upper cluster of seismicity that extends from 5 to 15 km and a lower cluster that extends from 20 to 35 km. Preliminary analyses of focal mechanisms (Wu and Rau 1998; Wu et al. 2004) indicate a complex zone of deformation but with many events recording left-lateral motions on NW-striking planes. The second pattern of seismicity developed in the few months after the Chi-Chi earthquake and occurs

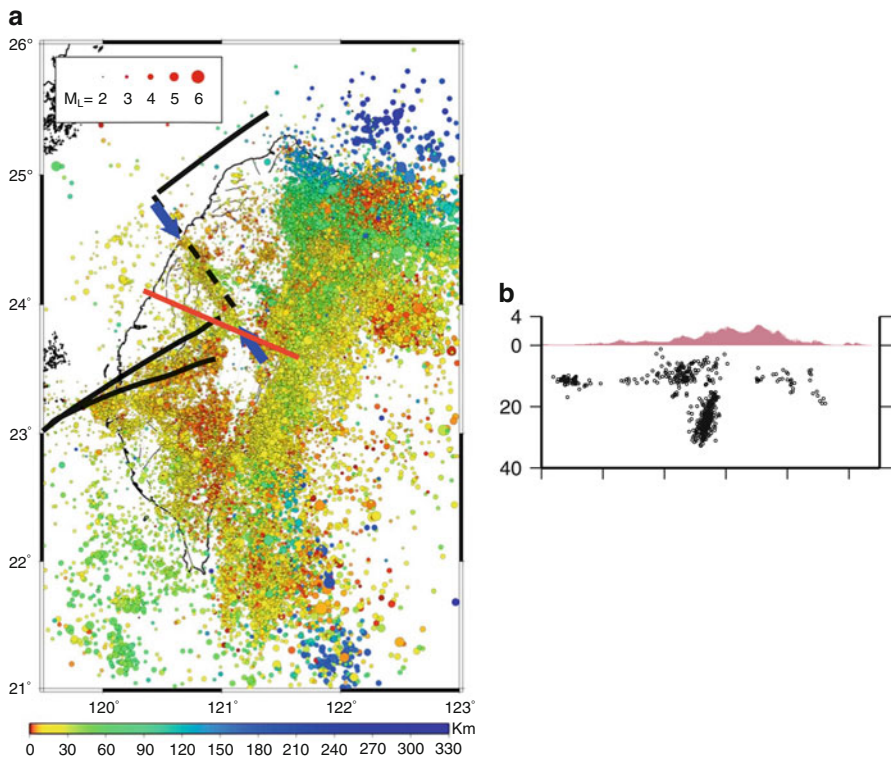

Fig. 8.7 (**a**) Pre- Chi-Chi seismicity (1990–1995; Lin et al. 2010) that shows Sanyi-Puli seismic zone (delimited with blue arrows) and seismicity along the southern edge of continental promontory. Note Sanyi-Puli zone parallels proposed continental margin facture zone (*dashed line*). (**b**) Post-Chi-Chi seismicity (20 Sept. 1999 to 31 Dec. 1999) along a vertical profile in central Taiwan (location shown in (**a**)) (from Wu et al. 2004). Note steeply west-dipping zone of seismicity in the middle of the section that correlates with the eastern edge of the promontory.

at the southeast end of the Sanyi-Puli zone (Fig. 8.7b). This zone also extends to nearly 40 km. The pattern of seismicity defines a planar, steeply west-dipping zone and focal mechanism solutions yield mostly top-to-the-east, or thrust, sense of slip (Wu et al. 2004). This cluster correlates spatially with the proposed eastern corner of the continental margin (Fig. 8.7b). The third seismic pattern occurs along the southeast edge of the magnetic anomaly and could equally be described as a seismic–aseismic transition in map view. This zone trends slightly oblique to the structural grain of the fold-and-thrust belt but parallel to the trend of the rifted margin (Fig. 8.7a) (Lin et al. 2003). This seismic–aseismic transition is present in both pre- and post-Chi-Chi data. Earthquakes south of the magnetic anomaly are relatively shallow (<20 km) and have a variety of focal mechanism solution, although Hsu et al. (2008) has recently proposed that the dominant focal mechanism solutions in this area changed from mostly strike-slip to most normal before and after the Chi-Chi earthquake. Taken together these zones of seismicity define a triangular zone in central Taiwan with relatively low seismicity, which approximates the boundary of the proposed continental margin promontory (Fig. 8.7a).

In addition to the clusters of seismicity that define the perimeter of the promontory, the distribution and magnitude of co-seismic slip associated with the 1999 Mw 7.6 Chi-Chi earthquake also correlate with the promontory (Fig. 8.8). The surface rupture of the Chelungpu fault, which slipped during the earthquake, generally trends north–south, slightly oblique to the structural grain of the orogen. Figure 8.8a shows the distribution of slip greater than 1 m based on GPS data

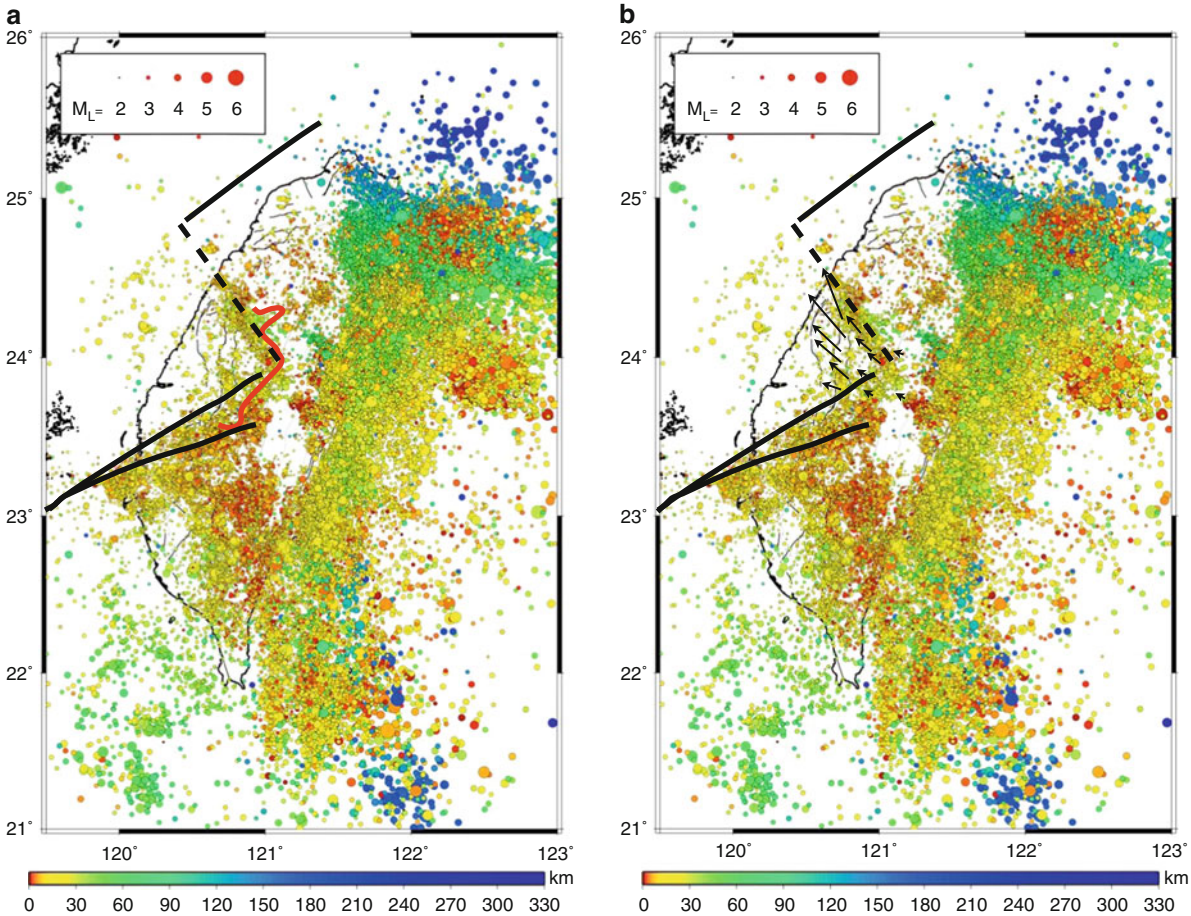

Fig. 8.8 Co-seismic slip associated with the 1999 Mw 7.6 Chi-Chi earthquake based on GPS data (Yu et al. 2003; Hsu et al. 2003). (**a**) *Curved line* shows distribution of area that slipped greater that 1 m (Hsu et al. 2003) and (**b**) *arrows* show representative slip vectors (Yu et al. 2003).

(Yu et al. 2003; Hsu et al. 2003) overlain on the proposed interpretation of the continental margin. Although irregular, the 1 m contour generally follows both the southeastern and northeastern boundaries of the promontory. The magnitude of co-seismic slip also varies systematically across the promontory. In the southern end of the Chelungpu fault, near field displacements are about 1.5 m. whereas at the north end of the fault, displacements are greater than 10 m (Yang et al. 2000). This along-strike increase in displacements correlates with the increase in width of the promontory (Fig. 8.8b), measured parallel to the plate convergence vector. One possibility, therefore, is that the geometry of the promontory limited the area of pre-elastic strain accumulation as well as subsequence seismic displacements.

The earthquake also illuminated a steeply dipping, planar zone of seismicity southeast of the Chelungpu fault a few hours after the main shock (Wu et al. 2004). Seismicity started near the southern end of the Chelungpu rupture, in the area of the previously recognized Luliao fault zone (Lee et al. 1999; Wu et al. 2004), and propagated southeast for about 50 km, crossing geologic boundaries at an acute angle (Fig. 8.9). The seismicity extends to 12–13 km and is dominated by left-lateral focal mechanisms (Wu and Rau 1998). The Luliao seismic zone therefore has the geometric and kinematic characteristics of a tear fault

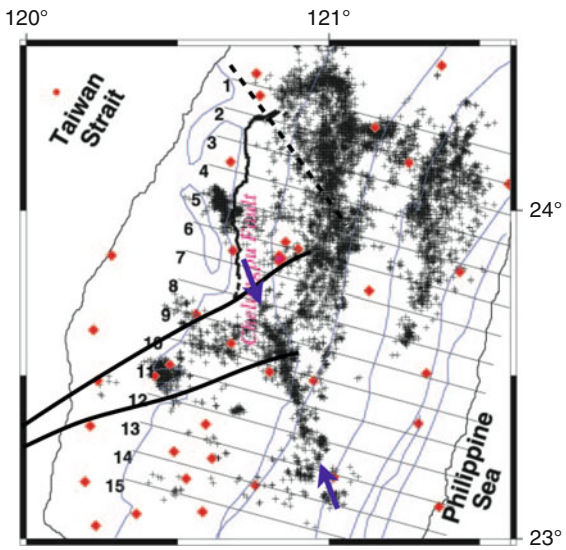

Fig. 8.9 Post-Chi-Chi seismicity in central Taiwan showing the Luliao seismic zone (*blue arrows*) (from Wu et al. 2004). *Black lines* = geologic boundaries.

in the fold and thrust belt, although the southeastern end of the zone extents into the slate belt, which overlies the edge of the Peikang High in this area. The zone also generally correlates with the edge of the Taishi Basin and is broadly equivalent to the previously recognized Pakuashan transfer zone (Mouthereau et al. 2002; Deffontaines et al. 1997).

Island-wide kinematics interpreted from focal mechanisms also appear to reflect collision with the promontory. Yeh et al. (1991), using earthquakes prior to 1987, recognized a regional fanning of the trend of $\sigma 1$ from NW in northern Taiwan to SW in southern Taiwan and proposed that reflected collision with the Peikang high. Rau and Wu (1998), using a larger data set, documented a relatively heterogeneous stress field throughout Taiwan with thrust faulting common in the fold and thrust belt and strike-slip and normal faulting in more common in the Central Range. They also suggested that strike-slip faulting was unusually common around the Peikang high. Wu et al. (2004) and Hsu et al. (2008) confirmed many of these patterns and emphasized the importance of both deep and shallow normal faulting in the Central Range.

Finally, a generally aseismic area, both pre- and post-Chi-Chi, occurs in the higher elevations (>1,500 m) of the Central Range between the continental margin promontory and the arc (Fig. 8.10) (Wu et al. 2004, 2007; Hsu et al. 2008). Hsu et al. (2008) also noted that focal mechanisms of earthquakes just to the northeast and southwest of this aseismic zone are dominantly extensional. They (Hsu et al. 2008) proposed that this along-strike change in seismicity reflected an along-strike change in the magnitude of horizontal stresses with a constant vertical stress. That is, they proposed that at elevations >1,500 m $\sigma 1$ is vertical and that the area of aseismicity is an area of high horizontal stress, relative to the areas of extension to the north and south. This interpretation is consistent with our proposal that the continental margin promontory is colliding with the arc in the area of high horizontal stresses (Fig. 8.10), which appears to limit extensional failure in this area.

8.6.2.2 Global Positioning System (GPS) Displacements and Strain

Yu et al. (1997) conducted an island-wide survey from 1990 to 1995 that produced the first comprehensive

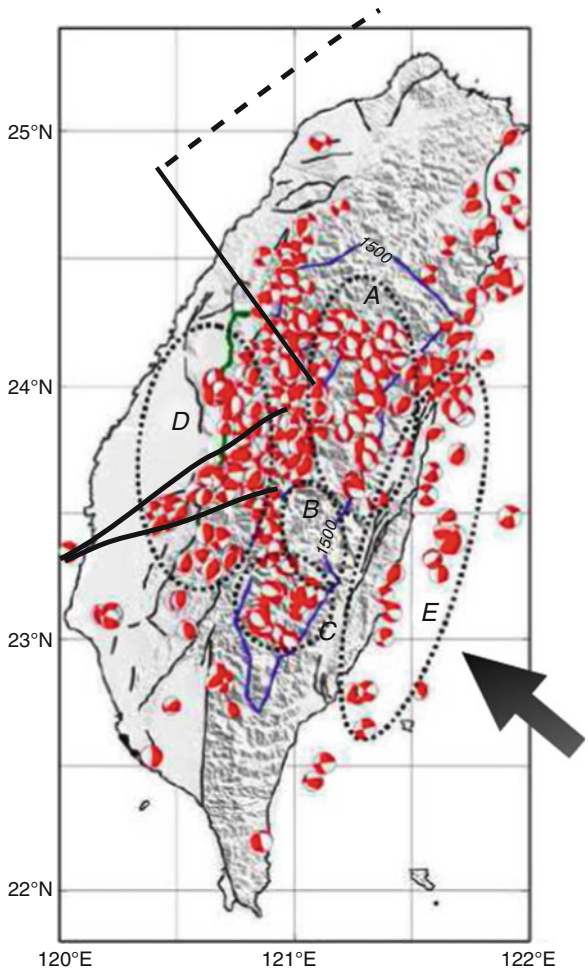

Fig. 8.10 Seismicity and focal mechanisms between July 1999 and July 2001 (i.e., mostly after the Chi-Chi earthquake) (from Hsu et al. 2008) showing aseismic zone at elevations >1,500 m (*blue line*). with extensional focal mechanisms to northeast and southwest. Areas: A = mostly normal faulting; B = aseismic; C = normal faulting and strike-slip; D and E = mostly thrusting with σ_1 northwest-trending.

view of surface deformation across Taiwan. Their data confirmed the wide distribution of deformation associated with the collision and illuminated a fanning of velocity vectors around a basement high in west-central Taiwan (Fig. 8.11a). Geological and geophysical data as well as physical and numerical models seemed to confirm the importance of this high in the deformation of the Taiwan orogen (Lacombe et al. 2001, 2003; Lu and Malavieille 1994), although it remained poorly defined.

Several authors have used the 1990–1995 GPS data (Yu et al. 1997) to examine different aspects of the collision (e.g., Chang et al. 2003; Bos and Spakman 2003), including Chang et al. (2003) who re-calculated the velocity field (using a linear interpolation algorithm) to map strain rate tensors over an approximately 11 km grid. Chang et al. (2003) also mapped the ratio of the two horizontal strain rate components at each grid node (Fig. 8.11b). For example, 100% extension means both strain rates are extensional whereas 100% compression means both strain rates are compressional. A strike-slip regime would have strain rates of opposite sign.

The resulting deformation mode map (Fig. 8.11b) shows two dominant belts – a western belt of compression in the fold-and-thrust and an eastern belt of extension in the Central Range. A less prominent belt of compression also occurs in the Coastal Range, which, in the central part of the range, expands westward nearly crossing the Central Range and linking up with compression belt in the west. The western and eastern belts are also composed of sub-domains; two sub-domains of compression in the west and three sub-domains of extension in the east, separated by a narrow zones of strike-slip deformation. The northern zone of compression overlies the western deformation front of the Hsüehshan Range whereas the southern zone, which is nearly twice as wide, overlies the southern fold and thrust belt and fills the triangle zone of the proposed continental margin promontory. The northern sub-domain of extension probably reflects westward propagation of the Okinawa Trough into the Central Range whereas the two southern sub-domains of extension correlate with the extensional zones at high elevations in the Central Range recognized by Hsu et al. (2008), although the southern sub-domain extends slightly further south. In any case, the correlation between the large zone of compression in southwestern Taiwan with the proposed continental margin promontory shows that it strongly influences deformation within the orogen.

The west to southwest fanning of the GPS vectors in southern Taiwan is perhaps one of the most striking features of the GPS data. Yu et al. (1997) proposed that the fanning reflected deflection and possibly extrusion of the orogen to the southwest as it collided with the Peikang High. Subsequent analysis and additional data confirmed the importance of the high in deflecting the orogen (e.g., Gourley 2006; Hickman et al. 2002; Angelier et al. 2009; Ching et al. 2007), although the geometry of the extruding block was not

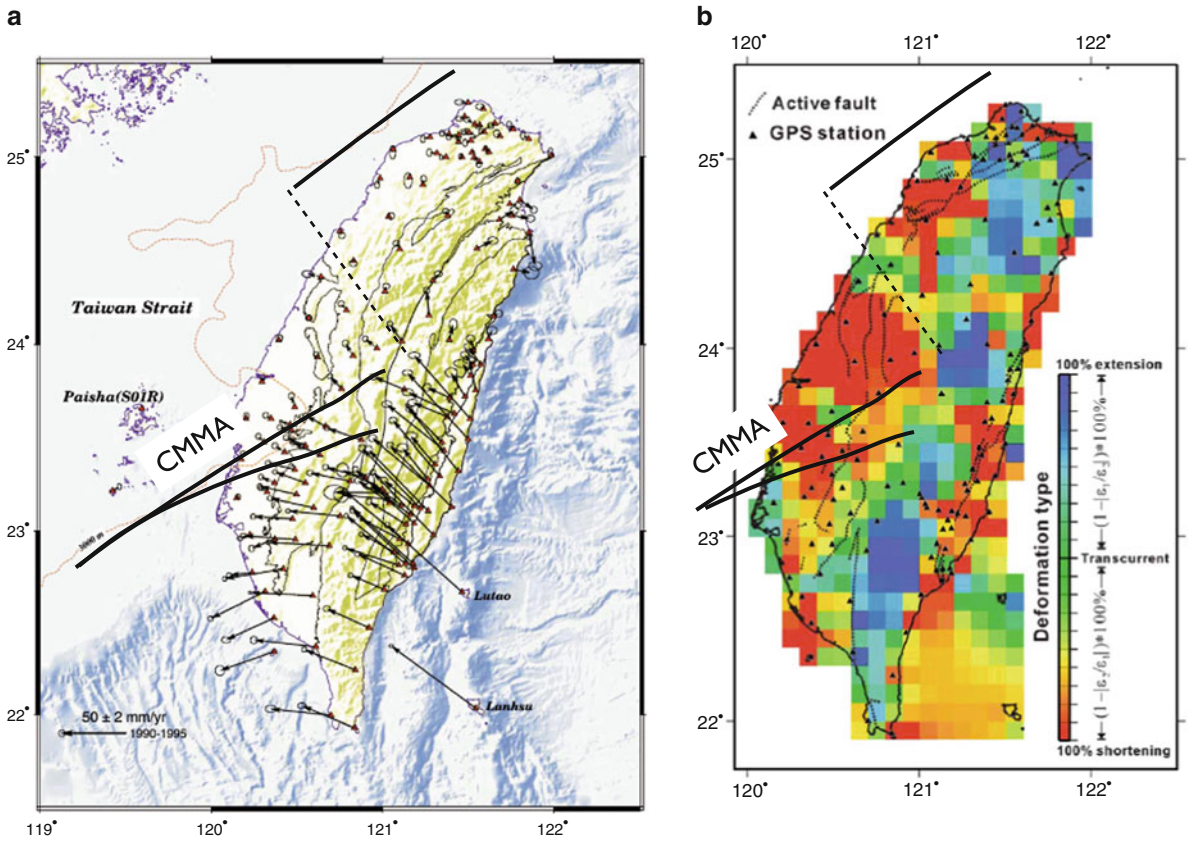

Fig. 8.11 (**a**) GPS displacements from 1990 to 1995 (from Yu et al. 1997) and (**b**) deformation modes (from Chang et al. 2003) based on data shown in (**a**). Displacements in (**a**) are relative to Penghu Island (station S01R), located in the Chinese continental margin.

well defined. To elucidate the extruding block, particularly the block boundaries, we re-plotted the vectors referenced to the central part of the Central Range (Fig. 8.12); that is, relative to a reference frame close to arc and opposite the continental margin prong. In this frame of reference, the GPS displacements in southern Taiwan show general flow of the upper crust to the southwest at about 3–5 cm per year. This regional-scale southwest flow is associated with right-lateral displacements on the west in the area of the Chishan fault and left-lateral displacements on east in the area of the western Central Range (Fig. 8.12). Left-lateral shear in the western Central Range is also associated with significant extension; thus, this zone may be a zone of left-lateral transtension.

Since the Chi-Chi earthquake, over 300 permanent GPS stations have been installed throughout Taiwan, providing continuous, island-wide coverage for the first time (Lin et al. 2010) as well as more detailed insights into the collision kinematics. Lin et al. (2010) used continuous GPS data collected from 110 stations from 1 January 2003 to 31 December 2005 characterized the surface deformation after the 1999 Chi-Chi earthquake. At the broadest scale, these data confirm the importance of the continental margin promontory as defined by the truncated magnetic anomaly and the Sanyi-Puli seismic zone. The strain rate data also show the three areas of extension identified by Chang et al. (2003) and Yu et al. (1997) and more clearly define the band of compression between the promontory and the Coastal Range (Fig. 8.13a). The eastern and western boundaries of the extruding block in southern Taiwan also display clockwise and counterclockwise rotational strains, respectively, consistent with regional-scale lateral flow of at least the upper crust (Fig. 8.13b). The post-Chi-Chi GPS displacement data, when

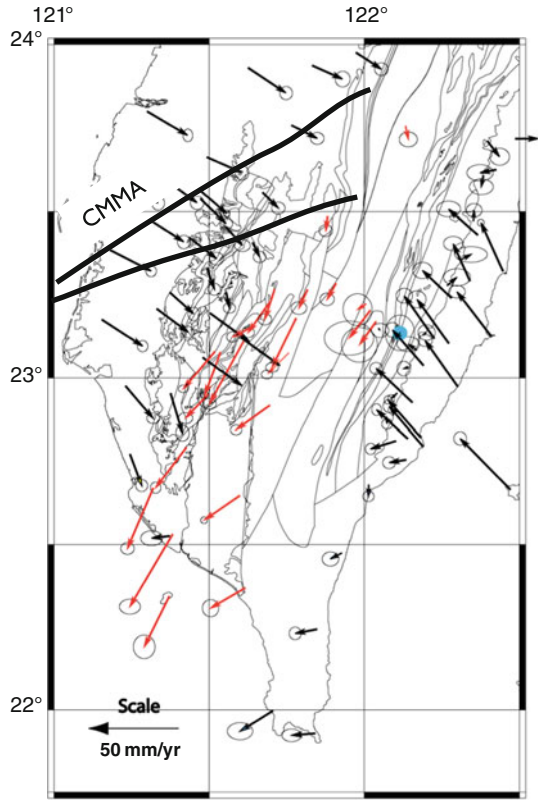

Fig. 8.12 GPS displacements from Yu et al. (1997) and Hickman et al. (2002) plotted with respect to a reference frame in the eastern Central Range (*blue dot*).

compared to the pre-Chi-Chi data, also show significant displacements in Central Range southeast of the area that moved during the 1999 Chi-Chi earthquake (Fig. 8.14) (Lin et al. 2010), suggesting that post-seismic processes are still active (Hsu et al. 2007). Lin et al. (2010) propose that these relatively large post-Chi-Chi displacements may reflect a viscoelastic response or afterslip of the Chi-Chi earthquake (e.g., Perfettini and Avouac 2004; Hsu et al. 2007). In any case, these displacements occur between the promontory and arc, the area of higher horizontal compression, which is consistent with our proposal that the promontory plays a critical role in the dynamics of the orogen.

8.6.2.3 Topography

Detailed studies of the topography along the length of the orogen show significant anomalies in the context of a propagating steady-state orogen. In one of the earliest quantitative studies of the topography of the Central Range, Willemin and Knuepfer (1994) showed that the middle part of the range is narrower, shorter and steeper than the range to the north and south (Fig. 8.15). Suppe (1981) also recognized the narrowing of the range in this area, but proposed that overall the orogen maintained an average width of 90 km throughout its length. More recently, however, Stolar et al. (2007a) quantified the topographic variability in the portion of the Central Range conventionally thought to be in steady state and found that variations in mean elevation and cross-sectional area are significant – up to 30% of the mean value. The anomalies correspond to the Hsüehshan Range in the north and to the continental promontory in central Taiwan. At smaller scales, Wobus et al. (2006) and Stolar et al. (2007a) have documented ubiquitous hanging tributary valleys and knickpoints along major rivers in the eastern Central Range, indicating a combination of non-uniformity and transience in the tectonic and erosional forcing of the Central Range landscape. Shyu et al. (2006) have also been mapped several thrust faults by along the eastern range front in the central part of the range. Despite uncertainty about the age of faulting, these observations imply that tectonic activity is, or has been recently, higher in the middle part of the range than in the south, which is opposite from predictions of the southward propagation model.

8.6.2.4 Penetrative Fabrics

One of the most prominent features of the Central Range is a penetrative, slaty cleavage that forms a fan across the range (Fig. 8.16) (e.g., Stanley et al. 1981; Crespi et al. 1996; Fisher et al. 2002; Ho 1988). On the western flank of the range the cleavage dips east and is associated with top-to-the-west asymmetric structures (e.g., folds, thrusts and shear zones). On the eastern flank, the cleavage dips west, asymmetric structures appear to be overturned, and the cleavage is often overprinted by a second or third crenulation (Fisher et al. 2002). Although the origin of cleavage fan is undoubtedly complex (Yeh et al. 2001; Fisher et al. 2002, 2007; Pulver et al. 2002), a recent compilation of cleavage data from the range (Fig. 8.16) (Lu et al. 2010) shows that the apex of the fan (i.e., where the cleavage has vertical dip), consistently lies just east of the ridge crest nearly the entire length of the

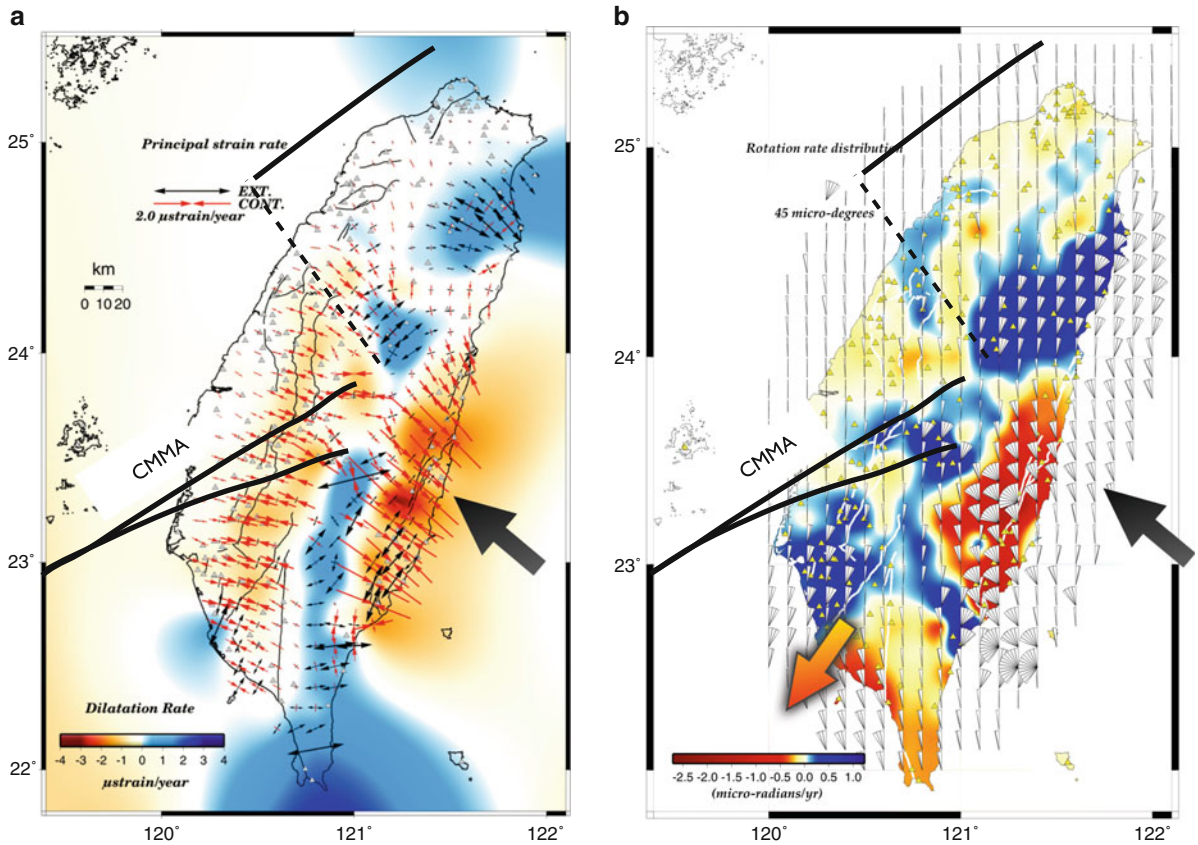

Fig. 8.13 (**a**) Dilatational and (**b**) rotational strain rate data from continuous GPS data collected after the 1999 Chi-Chi earthquake (2003–2005) (Lin et al. 2010).

orogen. This consistency is maintained even in the central section of the range where the range is anomalously steep and narrow (described above).

Topographic development is normally considered to be relatively young, especially in Taiwan where uplift and exhumation rates are relatively high, and slaty cleavage is normally considered to form substantially deeper in the crust (e.g. at depths equivalent to 200° to 300°); thus, the correlation of the cleavage geometry with the topographic crest is unexpected. With the available data, several interpretations are possible: (1) The slaty cleavage formed at earlier stage of the orogen whereas the fan of cleavage formed contemporaneously with the topography; (2) Both the cleavage and cleavage fan formed during an earlier stage of the collision and were subsequently deformed as the topography developed; (3) The cleavage and the cleavage fan formed at relatively shallow structural levels (e.g., due to anomalously high heat flow) and at about the same time as the topography. Although we are not able to eliminate any of these possibilities, the consistency between the cleavage fan and the topography argues that the topographic anomaly reflects a crustal-scale processes, suggesting the continental margin promontory is driving both the tectonic and topographic evolution.

8.6.2.5 Crustal-Scale Structure, Thickening and Exhumation

The crustal-scale structure in the central part of Taiwan provides additional constraints on the evolution of the orogen and the role of the promontory. A variety of geophysical tools have been used to understand the three-dimensional structure (e.g., Wu et al. 2004, 2007; Cheng 2004; Kim et al. 2005) and the structure of orogen appears to be relatively complex (compare e.g., Wu et al. 1997; Willett et al. 2003; Simoes et al. 2007; Suppe et al. 2010). We start

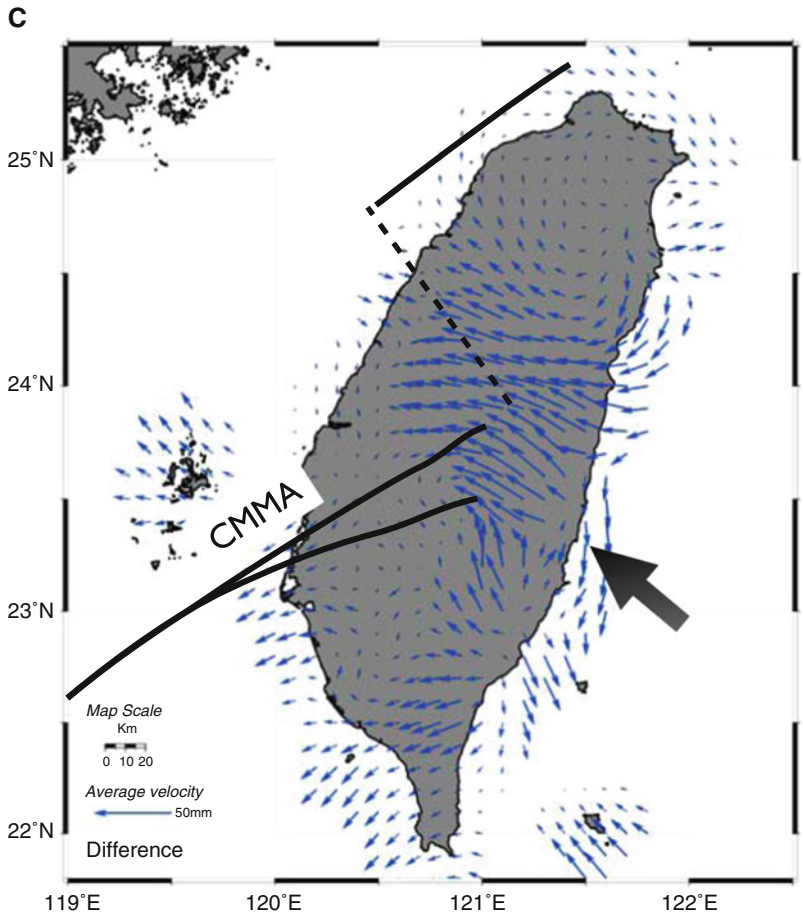

Fig. 8.14 Difference between GPS velocities collected before (from 1990 to 1995) and after (2003 to 2005) the Chi-Chi earthquake in terms of average annual velocity (from Lin et al. 2010).

with a recent interpretation of the crustal thickness (Wang et al. 2010a) and then examine horizontal sections of the P-wave velocity in the middle and lower crust which will then be complemented with higher resolution vertical cross-sections of seismic wave velocity and attenuation models. This compilation suggests that an area of thickened crust with relatively high P- and S-wave attenuation lies between the colliding continental margin promontory and the volcanic arc.

Wang et al. (2010a) recently analyzed receiver functions from the "Broadband Array in Taiwan for Seismology" catalog to estimate variations in crustal thickness (H) and Vp/Vs ratio (k) in the collision. Waveforms and travel times of 220 carefully selected teleseismic events and a two-stage weighted stacking process were used to reduce errors and increase the signal-to-noise ratio. In fact, high quality receiver functions can provide higher resolution H values than seismic tomography, which often yields higher resolution images of the crustal interior. The receiver function results suggest two viable models. One model, preferred by Wang et al. (2010a), shows the Moho as a 52 km deep elongate depression with gradients that cuts across the orogen at nearly right angles, including the Puli embayment and the Hsüehshan Range. The second model shows a shallower maximum depth for the Moho (~40 km in central Taiwan) and more uniform crustal thicknesses beneath the Central and Hsüehshan Ranges. We prefer this second model (Fig. 8.17a) because the uniform crustal thickness beneath the main ranges is more consistent with P-wave and gravity inversions. Both models, however, show the thickest crust in central Taiwan, primarily between the promontory and the arc, with thinner crust to the north and moderately thick crust to the south.

The relatively thick crust in central Taiwan is consistent with P- and S-wave velocity inversions and gravity data. For example, Cheng (2004) preformed a sequential inversion of travel-times and gravity data to image the three-dimensional velocity structure in

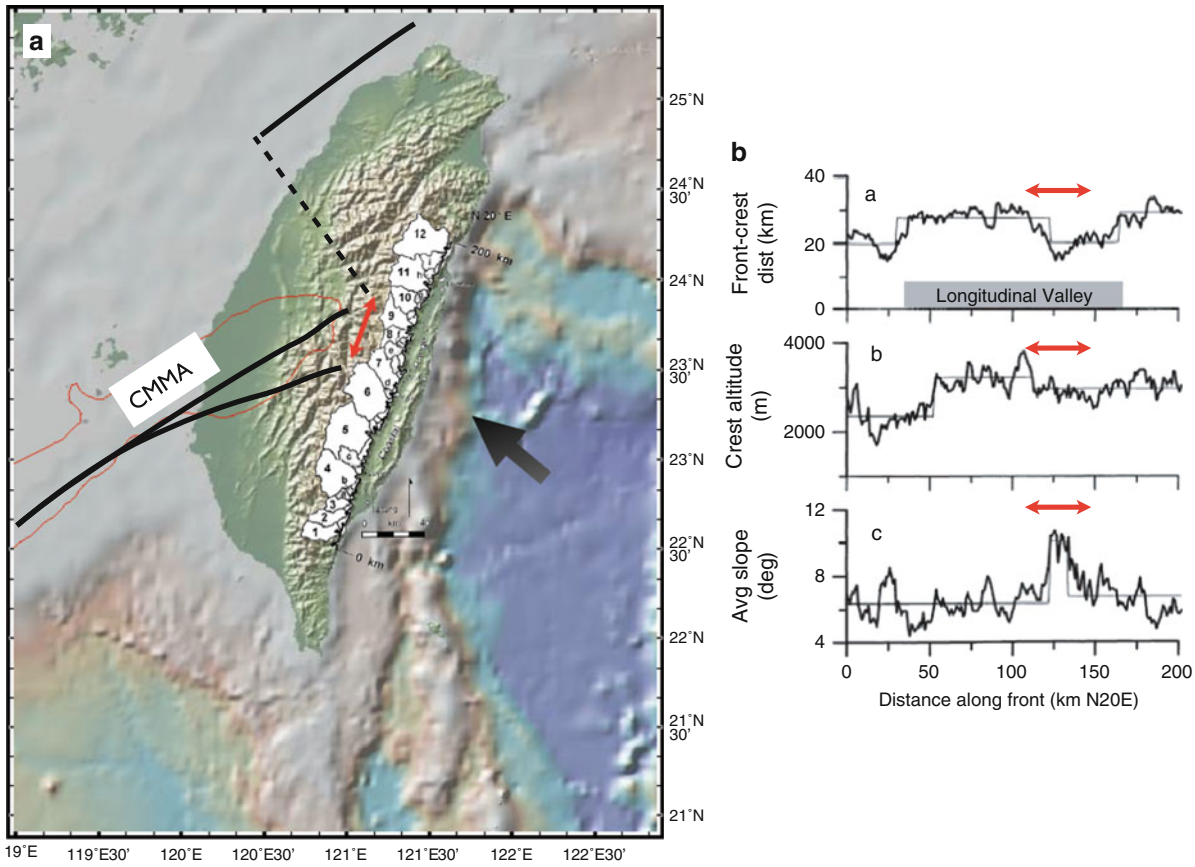

Fig. 8.15 (**a**) Watersheds and (**b**) along-strike variations in critical geomorphic parameters along the eastern flank of the Central Range (from Willemin and Knuepfer 1994). *Red double arrow* shows same along-strike section in (**a**) and (**b**).

central Taiwan. His results show an elongated "S" shaped low velocity zone at a depth of 25 km (Fig. 8.17b). The northern segment of the "S" lies beneath the Hsüehshan Range whereas the southern segment is much wider and extends beneath parts of both the Alishan and Central Ranges in central Taiwan. Kim et al. (2005) and Wu et al. (2007) obtained broadly similar results using P-wave tomography.

Wu et al. (2009) recently completed a high resolution study of the velocity structure in northern Taiwan and their results show confirm the presence of a low-velocity zone beneath the Hsüehshan Range (i.e., the northern segment of the "S" in Fig. 8.18a). In addition, their data show that the low velocity zone dips east about 45° to a depth of about 60 km (Fig. 8.18a). This east-dipping crustal layer was also identified by Lin and Roecker (1993) using the Vp tomography of Roecker et al. (1987) and carefully selected arrival times of P and S waves. Finally, recent attenuation models of the crust in northern Taiwan using both P- and S-waves (i.e., Qp and Qs) also confirm the moderate east dip (Fig. 8.18b) and show that the east-dipping zone of low Vp correlates with a zone of high Qp (i.e., low attenuation), which is overlain by a zone of low Qp and high Vp (Fig. 8.18).

At a more regional scale, P-wave attenuation data (Wang et al. 2010b) show a well-developed high Q zone at 19 km in the area of the proposed promontory and low Q zones beneath the Hsüehshan Range and in the central part of the Central Range (Fig. 8.19). The low Q zones wrap around the northern and eastern sides of the promontory and mimic the low velocity mid-crust identified by Cheng (2004). Wang et al. (2010b) interpret the low Q values in the Hsüehshan and Central Ranges to be related to recent and relatively rapid exhumation. Lee et al. (2010) (see also Lee et al. 2009) also completed a more detailed study of the attenuation in the central part of the Central

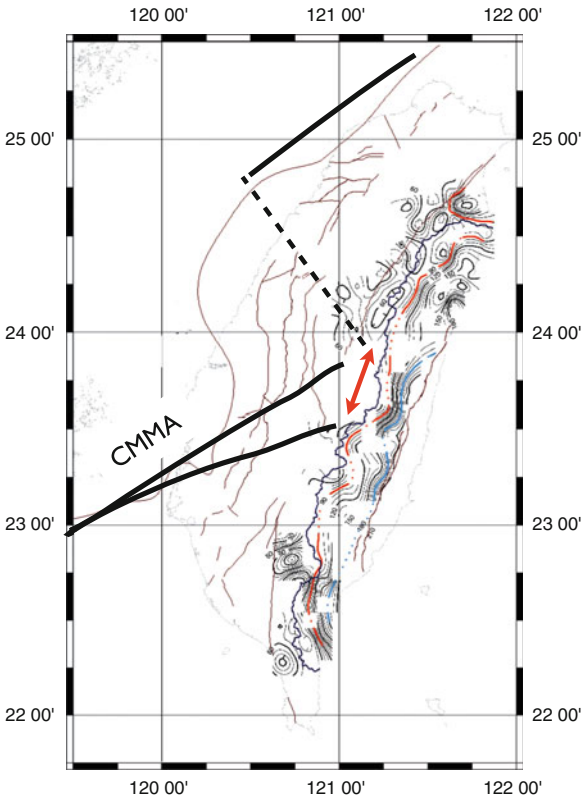

Fig. 8.16 Contour map of cleavage dip in the Central Range; *red line* = vertical dip; *blue* = overturned and horizontal cleavage (from Lu et al. 2010). *Black continuous line* just west of vertically dipping cleavage represents the topographic divide. *Red double arrow* is the same as in Fig. 8.15.

Range (box in Fig. 8.19) and show a low Q (high attenuation) zone that extends to 20–30 km. Using the observed attenuation values and published laboratory experiments, Lee et al. (2010) also estimated the temperatures in the area of the lowest Q values (~20 km depth) to be in the range of 680° to 750°C. These values are consistent with high heat-flow values (200–300 mW m^{-2}) measured by Lee and Cheng (1986) and suggest the possible presence of molten rocks at depth (Lee et al. 2010).

The area of high Q further southwest in the Central Range (Fig. 8.19) correlates with the outcrops of mafic rocks along the western boundary of the Tananao schists and may reflect the presence of more mafic blocks at depth. Cheng (2008) also recognized blocks of anomalously high velocity and density in this area (Fig. 8.5). That is, the along-strike change in attenuation in the Central Range (Fig. 8.19) may reflect changes in rock composition, rather than changes in the rate of exhumation.

In the southern most extent of the Central Range, velocity models and joint gravity-velocity inversions also suggest east-dipping crustal layers although relatively large blocks with anomalous density and attenuation values are also present. Cheng (2008) identified relatively thick crust (~30 to 40 km) in the southern Central Range, consistent with the receiver function analysis, and km-scale, east-dipping, high velocity layers. At least one of the layers projects to the surface near the Chaochou fault along the western Central Range. McIntosh et al. (2005) also recognized east-dipping high velocity layers in the southern Central Range using a geophysical survey that combined land and marine data.

8.6.2.6 Thermochronology and Exhumation

A number of studies have documented the complex thermal history recorded in the orogen since the early work of Lo and Onstott (1995) and Tsao (1996), including possible complications related to a continental margin promontory (e.g., Liu et al. 2001). For example, Liu et al. (2001; 1999), using completely reset detrital zircon grains, documented regional-scale patterns both across and along the structural grain of the orogen. These early data show younger exhumation cooling ages in the eastern Central Range and relatively older ages in the western Central and Hsüehshan Ranges. Liu et al. (2001) proposed that this orogen-scale pattern reflected different exhumation rates with relatively slow rates in the west (~1 mm per year) and much faster rates (~5 mm per year) in the east. More recent fission track data, much of which are compiled in Fuller et al. (2006), are consistent with this pattern; completely reset detrital zircon ages range from 6.4 to 2.9 Ma in the western Central Range range and from 3.0 to 0.8 Ma in the eastern part of the range. Reset detrital apatite ages and (U–Th)/He ages of zircons across are also consistent with a general decrease in the age of exhumation cooling east to west across the range.

Liu et al. (2001) also documented a single relatively old completely reset detrital zircon (~6 Ma, based on fission track) in southern Central Range that appeared to be anomalous in the context of southward propagation model. Liu suggested that this anomalous age might be related to collision of the Peikang high, although specific details on the geometry and timing were not provided. Relatively old completely reset apatite fission track ages have also

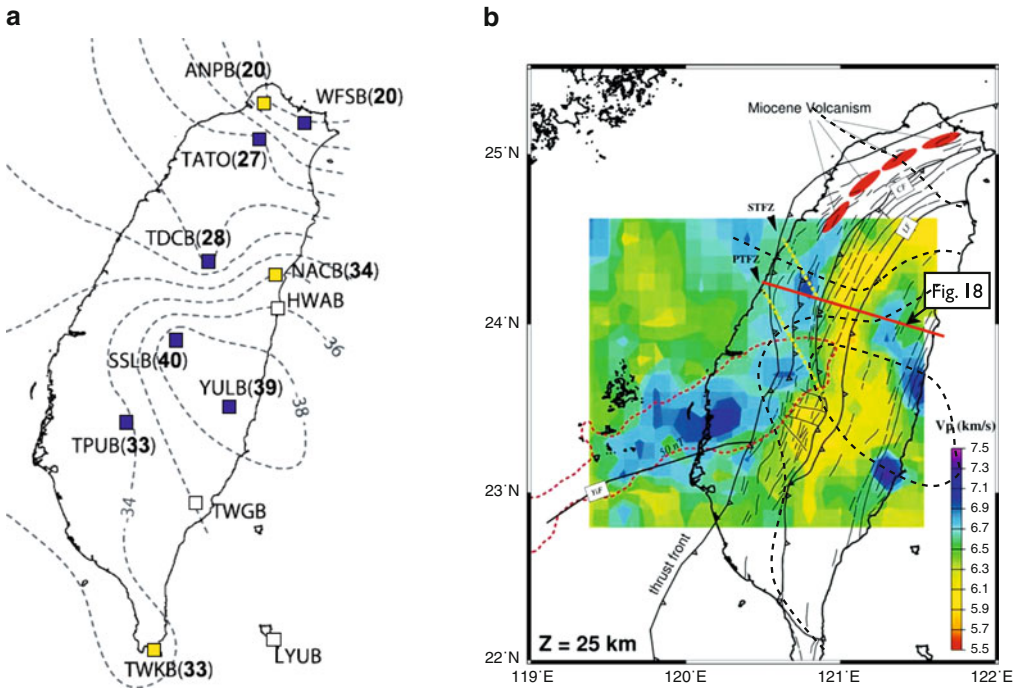

Fig. 8.17 (**a**) Depth to Moho beneath Taiwan (Wang et al. 2010a) and (**b**) P-wave velocity structure (at depth 25 km) in central Taiwan based a sequential inversion of travel-times and gravity data (Cheng 2004). Note the elongate "S" formed by the low-velocity crust centered on the promontory (*red dashed line* shows magnetic high) *dashed black lines* are the same as in (**a**).

been documented in southern Taiwan (Willett et al. 2003), supporting the early work of Liu et al. (2001). Willett et al. (2003) proposed a pre-collision thermal event, possibly related to burial on a relatively warm ocean floor or in an accretionary prism prior to the collision. More recently, Lee et al. (2006) used these older ages, as well as additional zircon fission track ages, to argue for a two-stage evolution of the orogen – an early accretion stage with relatively slow exhumation (evidenced by the older ages) followed by collision associated with faster exhumation (Fig. 8.6). Byrne et al. (2008) interpreted this temporal evolution in exhumation rates to a progressive collision rather than accretion followed by collision. In either case, the change in rates reflects fundamental changes in the processes supporting the orogen-scale topography.

8.6.2.7 Stratigraphic Record

Stratigraphic records preserved in the Western Foothills can also be used to interpret the history of the collision and are consistent with a multi-stage collision (Teng 1990; Chang and Chi 1983). In the Western Foothills, a basal unconformity separates an onlapping foreland basin sequence above from passive margin sequences below and marks the base of the Taiwan foreland sedimentation (Lin and Watts 2002; Yu and Chou 2001). In the Taishi Basin, Lin et al. (2003) estimated the age of the unconformity to be 6.5 Ma based on age-diagnostic fossil assemblages and a dated basalt layer 25 m beneath the unconformity. The foreland sediments generally record an upward increase in grain size and sediment accumulation rate reflecting, in part, the westward migration of the developing orogenic system and the progradation of orogenic sediments. In more detail, however, Chen et al. (2001) have documented an anomalously high sedimentation accumulation rates in both northern and southern Taiwan during the last 1.25 Ma (Fig. 8.20). From about 2.5 Ma to 1.25 Ma both areas record rates of ~900 m/m.y. At 1.25 Ma accumulation rates in northern Taiwan jumped nearly one order of magnitude to 900 m/100k years whereas in southern Taiwan the increase was less (~1,900 m/m.y.) but still substantially higher than typically measured in

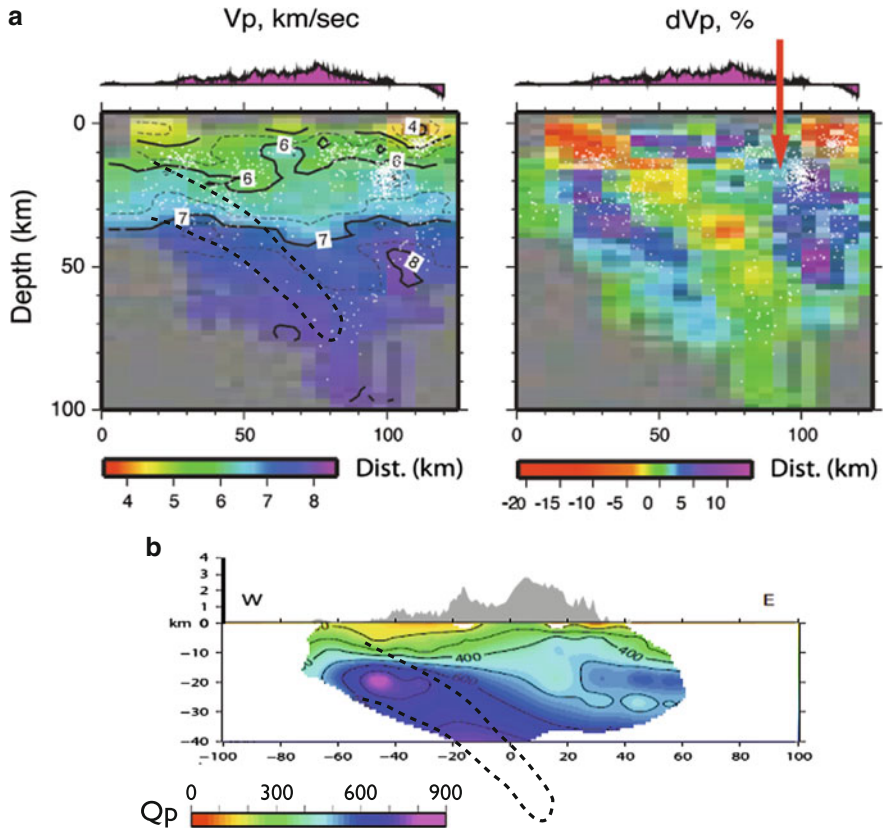

Fig. 8.18 Cross-sections showing contours of (**a**) Vp and dVp from (from Wu et al. 2009) and (**b**) P-wave attenuation (from Wang et al. 2010b); all at the same vertical and horizontal scales. Cross-section locations are shown in Figs. 8.17b and 8.19. *Dashed black line* in (**a**) and (**b**) is approximate distribution of low dVp.

foreland basins (e.g., 100–1,000 m/m.y., Jordon 1995). Although various interpretations are possible, the increase in accumulation rates correlate with the increase in exhumation cooling proposed by Liu et al. (2001) and substantiated with more extensive dating by Lee et al. (2006).

Simoes and Avouac (2006) also examined the spatial distribution of foreland sediments through time and proposed a southward propagation of the depositional center of the basin. Although Simoes and Avouac (2006) emphasized the southward propagation of the basins from 3.3 Ma to ~0 Ma, their data show that the basin was essentially stationary in northern Taiwan from 6.5 to 3.3 Ma. One possibility, therefore, is that this early foreland basin was constrained at its southern end, perhaps by a topographic or bathymetric barrier, and propagated southward only after this barrier was breached. In fact, a comparison of the reconstructed continental margin promontory suggests that this early foreland basin was constrained by the continental margin fracture zone. (Fig. 8.21).

Finally, the only two mélanges recognized in Taiwan appear to be sedimentary olistostromes that formed as the Central Range initially emerged above sea level. The Kenting and Lichi melanges crop out in the southern tips of the Central and Coastal Ranges, respectively, and contain distributed blocks of sandstone, shale, limestone (marble) and various compositions of igneous rocks, ranging from andesite to basalt, in a shale or mudstone matrix (Page and Suppe 1981; Page and Lan 1983; Chang et al. 2000; Huang et al. 1985; Tsan, 1974). The mafic igneous rocks in both units have also been interpreted to be remnants of ophiolites (e.g., blocks in the Lichi constitute the "east Taiwan ophiolite") (Page and Suppe 1981). Available fossil data indicate a limited range of age for the Lichi ranges (from 3.7 to 3.5 Ma) and a wider range for the Kenting (~10 Ma to <1 Ma) (Fig. 8.20)

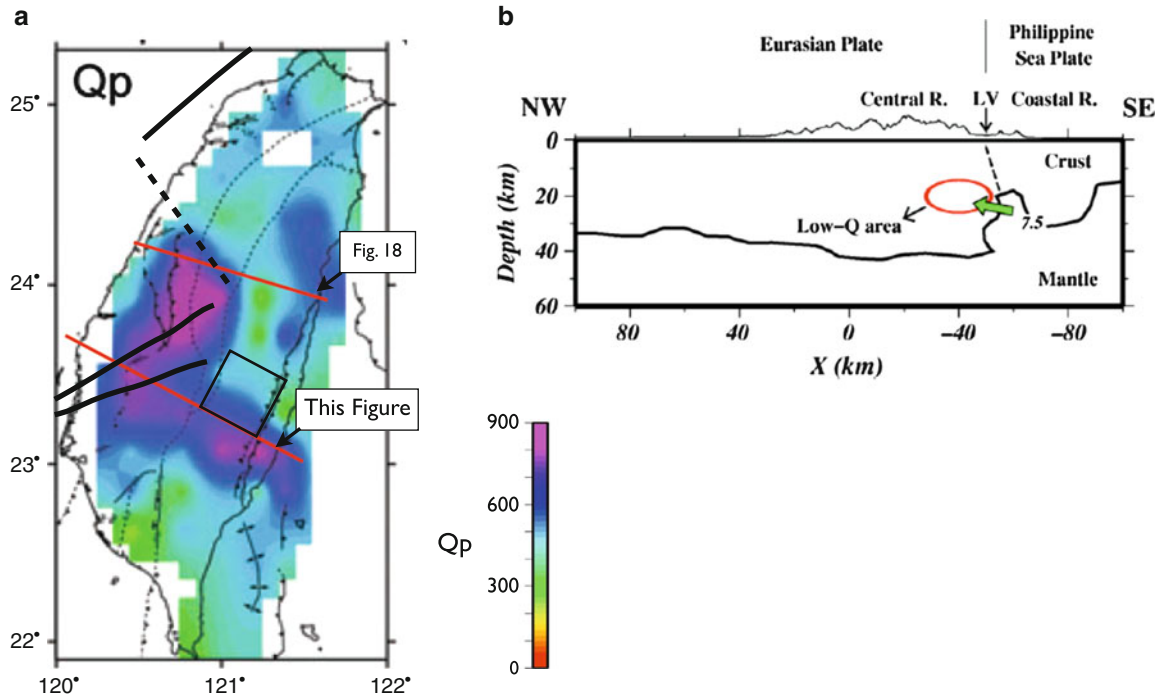

Fig. 8.19 (**a**) Map view of P-wave attenuation (at 19 km) from Wang et al. (2010b) and cross-section show (from Lee et al. 2010) showing the location of the low-Q zone (red ellipse) in a simplified crustal section (from Kim et al. 2005). Approximate Moho is shown by 7.5 km/sec contour.

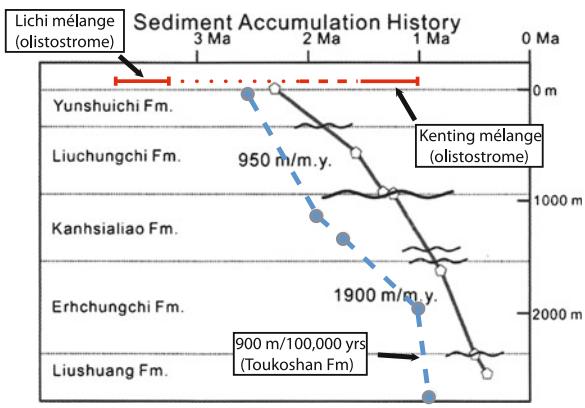

Fig. 8.20 Plot of sediment accumulation rates versus time in northern (*dashed blue line*) and southern stratigraphic sections (*gray line*) of the foreland basin (Tsaohuchi and Chengwenchi sections, respectively of Chen et al. 2001). *Wavy lines* show unconformities. Depositional ages of Lichi and Kenting olistostromes are shown for reference (see text for discussion).

(Huang et al. 2008; Chang et al. 2009). Page and Suppe (1981) carefully documented the age and stratigraphic relations of the Lichi mélange and showed that it stratigraphically interfingers with more coherent sedimentary units, confirming to these authors that the units are stratigraphic rather than tectonic. Page and Lan (1983) made the same argument for the Kenting mélange although the outcrop and stratigraphic relations were less clear. Huang et al. (1985), Huang et al. (2008) and Harris and Huang (2010) have proposed that both mélanges formed through tectonic processes or a combination of tectonic and diapiric processes (Harris and Huang 2010). Chang et al. (2000, 2009) showed, however, that although tectonic deformation substantially altered the original stratigraphy, the initial mixing of the various lithologies was the result of an olistostrome, as proposed by Page and Suppe (1981) and Page and Lan (1983). The low grade of thermal alternation ($< 100°C$) in both mélanges also indicates limited burial, consistent with their initial formation as olistostromes (see e.g., Byrne 1994). Both units are therefore interpreted to represent relatively large submarine slide deposits that formed as the Central Range and the magmatic arc emerged above sea level. The interpreted ages of deposition correlate with the proposed change in rates of exhumation cooling in the Central Range and with the increase in

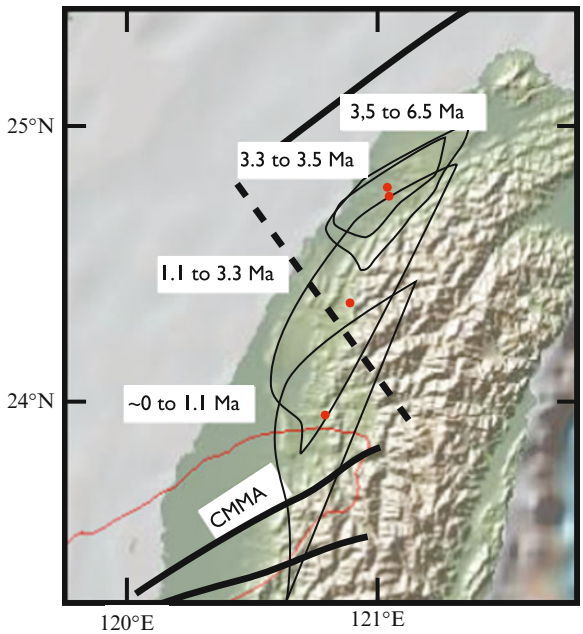

Fig. 8.21 *Black closed lines* show foreland basin depositional centers (from Simoes and Avouac 2006). Distribution of depositional centers suggests that the basin formed initially north of the proposed fracture zone (*dashed line*) and propagated southward as the arc collided with continental margin promontory.

rate of sediment accumulation in the foreland, suggesting the increase in rates of exhumation may have lead to at least local catastrophic failure and land sliding.

8.7 Discussion

Previous interpretations of the arc-collision in Taiwan have treated the Chinese continental margin as a relatively homogeneous passive margin that progressively collides with the arc (e.g., Byrne and Liu 2002a; Suppe 1984; Willett et al. 2003). Our compilation of a wide range of geological and geophysical data suggest, however, that the colliding passive margin was more heterogeneous than previously thought and that these heterogeneities have played, and continue to play, a significant role in the kinematics and dynamics of the orogen. The wide area of transitional crust southwest of Taiwan (~250 to 300 km across the margin) is consistent with geological data from Taiwan that indicate a relatively early history of accretion and exhumation (e.g., ~ 6 Ma to ~2 Ma). For example, if we assume that plate convergence (80 km/Ma) is partitioned approximately equally between shortening in the arc and deformation in the accretionary prism, as it is today, then during the last 3 m.y. (when the arc appears to have first rotated due to the collision) approximately 120 km of transitional crust could have been consumed through underthrusting in the prism. This results in between 130 and 180 km of transitional crust to be consumed prior to 3 Ma. Depending on the degree of partitioning between arc deformation and underthrusting in the prism, transitional crust may have first collided with the arc between 7.5 and 4.5 Ma (3 Ma plus 1.5 to 4.5). The rocks accreted during this early stage of the collision (7.5–4.5 Ma) are most likely exposed in the Hsüehshan and Central Ranges, or have been removed by erosion (e.g., the Taiwan ophiolite).

We propose that the late stage of the collision (~3–2 Ma to present) involved continental crust of more normal thickness (~30 km) and that this crust formed a regionally significant, and relatively rigid, continental promontory. Considering that the interpreted apex of the promontory still lies beneath central Taiwan, the volume of continental crust, of normal thickness, that has been underthrusted or subducted is fairly limited. Limited underthrusting of continental crust is also consistent with recent thermomechanical numerical models of the collision (Yamato et al. 2009). Although underthrusting of continental crust is interpreted to be relatively limited, the continental margin promontory and en echelon sedimentary basins north and south of it, appear to have dominated the growth of the orogen during the late-stage of the collision.

Perhaps the most conspicuous consequence of the colliding promontory is the map view curvature of the fold and thrust belt (Figs. 8.2 and 8.22) with a central zone of anomalously north-trending folds and thrusts. Our interpretation of this map-view curvature is that in southern Taiwan, thick continental crust of the promontory limited westward propagation of the fold and thrust belt; that is, the promontory acted as a buttress. In the north, the thick sedimentary sequences of the Taishi Basin allowed the thrust belt to propagate substantially west of the promontory, resulting in a left-lateral accommodation zone between the northern and southern thrust belts (Fig. 8.22). Left-lateral shear appears to be accommodated at deep structural levels by slip along the Sanyi-Puli seismic zone, which is reactivating a continental margin fracture. At shallow structural levels south of this zone, left-lateral shear is

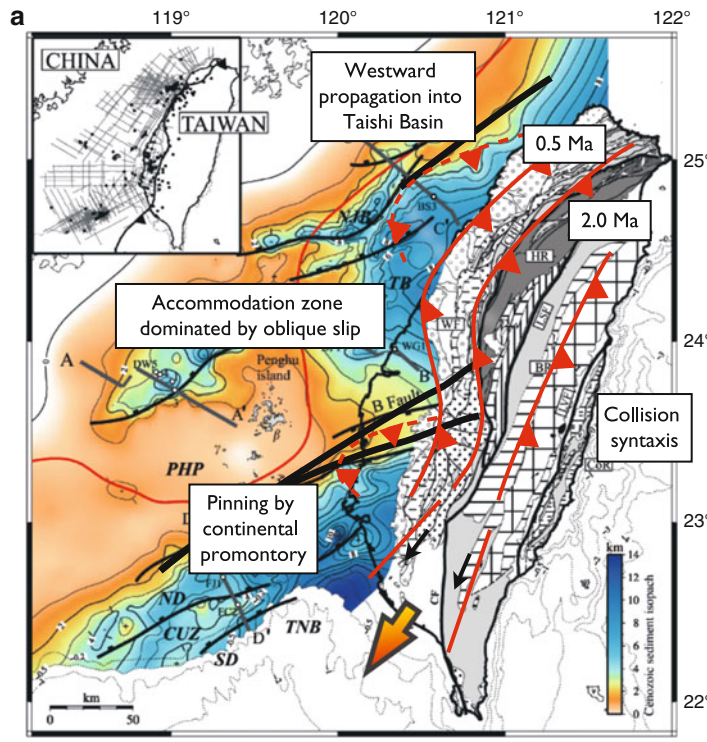

Fig. 8.22 Map showing depth to Mesozoic basement (Lin et al. 2003) and geology of Taiwan. *Red lines* with barbs show proposed development of Taiwan orogen from 2–3 Ma to present. *Dashed red lines* with barbs show are of reactivated normal faults (from Mouthereau et al. 2002). Ages are based on syn-tectonic stratigraphy in the central section of the fold-and-thrust belt. Note that the southern fold-and-thrust belt is in pinned by the continental margin promontory (*black line*) as the northern belt propagates northwest, resulting in an accommodation zone dominated by faults and folds with oblique slip. See Fig. 8.4 for abbreviations.

accommodated by the development of a thin-skinned fold and thrust belt in which slip is both oblique and partitioned along strike (e.g., see co-seismic slip during the Chi-Chi earthquake, Fig. 8.8). Geochronologic data from sedimentary basins between thrust sheets (i.e., "piggyback" basins) also document foreland propagation beginning about 2 Ma (Fig. 8.22) (Lee et al. 1996). If the slip pattern recorded during the Chi-Chi earthquake is representative of the long-term displacement, it would explain the progressive westward rotation of increasingly younger thrust sheets. In essence, the central Taiwan fold and thrust belt is interpreted to be a wide accommodation zone between thrust systems advancing at different rates. The southern boundary of this accommodation zone also appears to have been illuminated, at least in part, as the Luliao seismic zone just after the Chi-Chi earthquake (Wu et al. 2004).

The recognition of a continental margin promontory beneath central Taiwan and its correlation with a change in geometry of the fold and thrust belt in map view suggests that it may represent a recess or syntaxis in the fold and thrust belt. The correlation between the apex of the promontory and the thickest crust with the highest P-wave attenuation (e.g., compare Figs. 8.18 and 8.20) suggests that this should be an area of maximum rock uplift and exhumation, consistent with other orogenic syntaxes recognized around the world (Khan et al. 2000). This interpretation is also consistent with geomorphic indices from the central part of the Central Range that indicate high rates of uplift (Stolar et al. 2007b), with the absence of seismicity in this area (e.g., Hsu et al. 2008) and the presence of high heat flow (Lee and Cheng 1986). Although detailed thermochronologic and kinematic data are limited in central Taiwan, the available data suggest a recent increase in rates of exhumation consistent with the interpretation that the prong collided relatively recently (< 2 Ma).

The presence of a crustal-scale buttress in southern Taiwan and the collision of the continental margin prong may have also initiated lateral extrusion in the southern part of the orogen (Ching et al. 2007; Lacombe et al. 2001; Angelier et al. 2009). Again, detailed kinematic and geochronologic data are limited in this area of Taiwan, but two aspects of the available data suggest significant crustal involvement. First, GPS and geologic data suggest that extrusion is asymmetric with the western part of the extruding block being characterized by right-lateral transpression whereas the eastern part of the block is

characterized by left-lateral transtension (see e.g., Figs. 8.13 and 8.22). This asymmetry may reflect the regional-scale boundary conditions of east-dipping subduction and southwest-directed extrusion of the Central Range, suggesting that the extruding block involves the entire orogen from the décollement to the surface. In this context, transpression in the west reflects the combined effects of underthrusting and extrusion whereas transtension in the east reflects southwest-directed extrusion. Second, the area of transtension in the southern Central Range includes nearly the entire southern half of the Central Range (Fig. 8.13) with numerous peaks over 3,000 m. If the extensional regime indicated by the GPS (Yu et al. 1997) and brittle fault data (Crespi et al. 1996) is representative of relatively long-term rates (e.g., 3–2 Ma) then the surface topography must be supported by flow in the middle to lower crust. One possibility, therefore, is that crustal material flows from the syntaxis to the southwest. Again, suggesting involvement of at least the middle and upper crust.

Finally, the observations and interpretations presented above for the late-stage development of the orogen involve only limited southward propagation. Although paleomagnetically determined rotations in the arc show southward propagation, how this progressive collision-related propagation is transmitted into the orogen is less clear. In fact, available fission track ages indicate exhumation cooling began in both northern and southern Taiwan about 6 Ma (Liu et al. 2000, 2001; Lee et al. 2006). The southward migration of the foreland basin identified by Simoes and Avouac (2006) (Fig. 8.21) may also reflect the change in the depth of basement in the down-going plate from north to south, rather than propagation of the collision. For example, the foreland basin may have been restricted to the area of the Taishi Basin north of the continental margin fracture early in the collision and then propagated southward across the fracture zone and onto thicker crust as the continental margin promontory collided 2–3 Ma. Evidence for southward propagation also appears to be present in the southern Central Range (e.g., Willett et al. 2003; Wiltschko et al. 2010), but this may be a local response to crustal flow. For example, Ramsay et al. (2007), used geomorphic parameters and kinematic models from the southeastern flank of the range to argue for a rapid increase in rock uplift rates from the area of the orocline (Fig. 8.2) to about 23°N. One possibility, however, is that the increase in the rate of uplift, which increases towards the proposed orogenic syntaxis, is driven by lateral crustal flow away from the syntaxis. Fission track ages of completely reset detrital apatites from this area of the Central Range are consistent with this interpretation and suggest that the increase in the rate of uplift occurred about 2 Ma (Fig. 8.6) (Lee et al. 2006).

8.8 Summary

The compilation of a variety geological and geophysical data sets suggests that the Taiwan orogenic belt, which is often presented as a relatively simple, propagating orogen, has evolved in a least two stages and involved both lateral and vertical extrusion. The initial collision occurred between the Luzon arc and transitional crust of the South China Sea about 6 Ma. Based on observations from the South China Sea south of Taiwan the transitional crust was composed of thinned continental crust and newly formed mafic rocks. Rocks of similar composition are currently exposed in the Central Range of Taiwan and are inferred to be present at depth from seismic velocity data. The initial collision and accretion of transitional crust was followed by a more significant collision with a continental margin promontory of more normal (~30 km) thickness. This later stage of the collision is still active.

The continental margin promontory, as revealed primarily by magnetic data and the distribution of seismicity before and after the Chi-Chi earthquake, is only partially subducted beneath Taiwan. In western Taiwan, the promontory divides the fold-and-thrust belt into three parts – a northern salient, a central fold-and-thrust belt that fans from northeast- to north-striking and a southern salient offset left laterally from the northern fold and thrust belt. The central fold-and-thrust belts, therefore, represents an accommodation zone between two fold-and-thrust belts. In the Central Range, the apex of the partially subducted promontory correlates with an area in the orogenic belt that is relatively, narrow, steep and low in elevation. This area also has anomalously high P- and S-wave attenuation, suggesting relatively high rates of exhumation. In southwest Taiwan, the promontory, previously recognized as the Peikang High, limited the westward propagation of the fold-and-thrust belt. As a result, shortening in southern Taiwan

has been accommodated by vertical and lateral flow of at least the middle and upper crust.

The classic model of Taiwan as a southward propagating orogen with space-time equivalence may therefore be too simple. Instead, the kinematics and dynamics of the orogenic belt appear to be dominated by the presence of a partially subducted continental margin promontory and associated fracture zone. This relatively rigid promontory forms the apex of an orogenic syntaxis in central Taiwan that divides the orogen both along and across strike, resulting in structural domains with distinct deformational patterns and histories. Future studies therefore might focus on defining these various domains and on understanding how they interact temporally and spatially.

Acknowledgements We are grateful to the many colleagues in Taiwan who have kindly shared their data and ideas, and helped with the numerous logistical challenges over the years. We also acknowledge and appreciate support from the Department of Geological Sciences at the National Taiwan University and the Institute of Earth Sciences, Academia Sinica. Support from the Fulbright Foundation (to Byrne) and the National Science Foundation (EAR0711353 and EAR0738979) is also gratefully acknowledged. The ideas and conclusions were improved through numerous discussions with Jon Gourley, Jon Lewis, Chung Huang, Dave Mirakian and Hao-Tsu Chu. The support and patience of the editors, Dennis Brown and Paul Ryan is greatly appreciated.

References

Angelier J, Hsu HT, Lee JC (1997) Shear concentration in a collision zone: kinematics of the active Chihshang fault in the Longitudinal Valley, eastern Taiwan. Tectonophysics 274:117–144

Angelier J, Chang T-Y, Hu J-C, Chang C-P, Siame L, Lee J-C, Deffontaines B, Chu H-T, Lu C-Y (2009) Does extrusion occur at both tips of the Taiwan collision belt? Insights from active deformation studies in the Ilan Plain and Pingtung Plain regions: Tectonophysics 466:356–376.

Bos AG, Spakman W (2003) Surface deformation and tectonic setting of Taiwan inferred from GPS velocity field. J Geophys Res 108(B10):2458–2476

Briais A, Tapponnier P, Pautot G (1989) Constraints of Sea Beam data on crustal fabrics and seafloor spreading in the South China Sea. Earth Planet Sci Lett 95:307–320

Briais A, Patriat P, Tapponnier P (1993) Updated interpretation of magnetic anomalies and seafloor spreading stages in the South China Sea – implications for the Tertiary Tectonics of Southeast Asia. J Geophys Res 98(B4):6299–6328

Byrne T (1994) Sediment melanges – an example of the interplay of deformation and diagenesis. In: Maltman A (ed) Geological deformation of sediments. Chapman and Hall, London, pp 239–260

Byrne T, Liu C-S (2002a) Geology and geophysics of an arc-continent collision, Taiwan, vol 358, Geological Society of America Special Paper. Geological Society of America, Boulder, CO

Byrne T, Liu C-S (2002b) Preface: introduction to the geology and geophysics of Taiwan. In: Byrne T, Liu C-S (eds) Geology and geophysics of an arc-continent collision, Taiwan, vol 358, Geological Society of America Special Paper. Geological Society of America, Boulder, CO, pp v–vii

Byrne T, Chan Y-C, Lee Y-H, Lee J-C, Rau R-J (2008) Reconstructing Taiwan: a new view of a classic Orogen. In: Geological Society of America, National Meeting, Houston, TX. Geological Society of America Abstracts with Programs. pp T82 321–324

Byrne T, Daniels M, Miller J (2009) Footwall geometry and topography in the Taiwan arc-continent collision. In: Geological Society of America Northeastern Section-44th Annual Meeting, Portland, Maine. Geological Society of America Abstracts with Programs, p 3

Carena S, Suppe J, Kao H (2002) Active detachment of Taiwan illuminated by small earthquakes and its control of first-order topography. Geology 30(10):935–983

Chamberlain RT, Shepard FB (1923) Some experiments in folding. Journal of Geology 31:490–512

Chang SL, Chi WR (1983) Neogene nannoplankton biostratigraphy in Taiwan and the tectonic implications. Petrol Geol Taiwan 19:93–147

Chang C-P, Angelier J, Huang C-Y (2000) Origin and evolution of a mélange: the active plate boundary and suture zone of the Longitudinal Valley, Taiwan. Tectonophysics 325:43–62

Chang CP, Chang T-Y, Angelier J, Honn K, Lee J-C, Yu S-B (2003) Strain and stress field in Taiwan oblique convergent system: constraints from GPS observation and tectonic data. Earth Planet Sci Lett 214:115–127

Chang CP, Angelier J, Huang CY (2009) Evolution of subduction indicated by melanges in Taiwan. In: Lallemand S, Funiciello F, Lallemand S, Funiciello F (eds) Subduction zone geodynamics. Springer, Berlin, pp 207–225. doi:10.1007/978-3-540-87974-9

Chapple WM (1978) Mechanics of thin-skinned fold-and-thrust belts. Geol Soc Am Bull 89:1189–1198

Chen C-H (2000) Geologic map of Taiwan. Central Geological Survey, Ministry of Economic Affairs, Taipei

Chen W-S, Ridgeway KD, Horng C-S, Chen Y-G, Kai-Shuan S, Yeh M-G (2001) Stratigraphic architecture, magnetostratigraphy, and incised-valley systems of the Pliocene-Pleistocene collisional marine foreland basin of Taiwan. Geol Soc Am Bull 113:1249–1271

Cheng W-B (2004) Crustal structure of the High Magnetic Anomaly Belt, western Taiwan and its implications for continental margin deformation. Marine Geophys Res 25 (1–2):79–83. doi:10.1007/s11001-005-0735-3

Cheng W-B (2008) Tomographic imaging of the convergent zone in Eastern Taiwan – a subducting forearc sliver revealed? Tectonophysics. doi:10.1016/j.tecto.2007.11.010

Chi WR, Namson J, Suppe J (1981) Stratigraphic record of plate interactions in the Coastal Range of eastern Taiwan. Memoirs Geol Soc China 4:491–530

Ching K-E, Rau RJ, Lee J-C, Hu J-C (2007) Contemporary deformation of tectonic escape in SW Taiwan from GPS observations, 1995–2005. Earth Planet Sci Lett 262:601–619

Chou H-C, Kuo B-Y, Chiao L-Y, Zhao D, Hung S-H (2009) Tomography of the westernmost Ryukyu subduction zone and the serpentinization of the fore-arc mantle. J Geophys Res 114. doi:10.1029/2008JB006192

Clark MB, Fisher DM, Lu C-Y, Chen C-S (1993) The Hsüehshan Range of Taiwan: a crustal-scale pop-up structure. Tectonics 12(1):205–217

Crespi J, Chan Y-C, Swaim M (1996) Synorogenic extension and exhumation of the Taiwan hinterland. Geology 24(3): 247–250

Dahlen FA, Barr TD (1989) Brittle frictional mountain building 1. Deformation and mechanical energy budget. J Geophys Res 94(B4):3906–3922

Dahlen FA, Suppe J, Davis D (1984) Mechanics of fold-and-thrust belts and accretionary wedges: cohesive Coulomb theory. J Geophys Res 89:10,087–10,101

Dana JD (1866) A textbook of geology. Theodore Bliss, Philadelphia

Davis D, Suppe J, Dahlen FA (1983) Mechanics of fold-and-thrust belts and accretionary wedges. J Geophys Res 88: 1153–1172

Deffontaines B, Lee J-C, Angelier J, Carvalho J, Rudant J-P (1994) New geomorphic data on the active Taiwan orogen: a multisource approach. J Geophys Res 99(B10):20,243–20,266

Deffontaines B, Lacombe O, Angelier J, Chu H-T, Mouthereau F, Lee CT, Deramond J, Lee J-F, Yu M-S, Liew P-M (1997) Quaternary transfer faulting in the Taiwan foothills: evidence from a multisource approach. Tectonophysics 274:61–82

Dorsey RJ (1992) Collapse of the Luzon volcanic arc during onset of arc-continent collision: evidence from a Miocene-Pliocene unconformity, eastern Taiwan. Tectonics 11: 177–191

Fisher DM, Lu C-Y, Chu H-T (2002) Taiwan Slate Belt: insights into the ductile interior of an arc-continent collision. In: Byrne TB, Liu C-S (eds) Geology and geophysics of and an arc-continent collision, Taiwan, vol 358, Geological Society of America Special Paper. Geological Society of America, Boulder, CO, pp 93–106

Fisher DM, Willett S, Yeh E-C, Clark MB (2007) Cleavage fronts and fans as reflections of orogen stress and kinematics in Taiwan. Geology 35(1):65–68

Fuller C, Willett SD, Fisher DM, Lu C-Y (2006) A thermomechanical wedge model of Taiwan constrained by fission-track thermochronometry. Tectonophysics 425:1–24

Gourley JR (2006) Syn-tectonic extension and lateral extrusion in Taiwan: the tectonic response to a basement high promontory. University of Connecticut, Storrs

Harris R, Huang C.Y, Linking melange types and occurrences with active melange-forming process in Timor and Taiwan, in Proceedings Annual Meeting, Geological Society of America, Denver, CO, 2010, Geological Society of America, p. Paper 49–41

Hayes DE, Taylor BR (1978) Magnetic anomalies. In: Hayes DE (ed) Geophysical Atlas of East and Southeast Asian Seas, vol MC 25, Map and Charts Ser. Geological Society of America, Boulder, CO

Hickman JB, Wiltschko DV, Hung J-H, Fang P, Bock Y (2002) Structure and evolution of the active fold-and-thrust belt of southwestern Taiwan from Global Positioning System analysis. In: Byrne T, Liu C-S (eds) Geology and geophysics of an arc-continent collision, Taiwan, vol 358, Geological Society of America Special Paper. Geological Society of America, Boulder, CO, pp 75–92

Ho CS (1975) An introduction to the geology of Taiwan – Explanatory text of the geologic map of Taiwan. Ministry of Economic Affairs, Taipei

Ho CS (1976) Foothills tectonics of Taiwan. Bull Geol Surv Taiwan 25:9–28

Ho CS (1982) Tectonic evolution of Taiwan: explanatory text of the geologic map of Taiwan. Ministry of Economic Affairs, Taipei, Taiwan, Republic of China

Ho CS (1986) A synthesis of the geologic evolution of Taiwan. Tectonophysics 125:1–16

Ho CS (1988) An introduction to the geology of Taiwan – explanatory text of the geologic map of Taiwan, 2nd edn. Ministry of Economic Affairs, Taipei, Taiwan, Republic of China

Hsu S-K, Liu C-S, Shyu C-T, Liu S-Y, Sibuet J-C, Lallemand S, Wang C, Reed DL (1998) New Gravity and Magnetic Anomaly Maps in the Taiwan-Luzon Region and their Preliminary Interpretation. Terr Atmos Ocean Sci 9(3):509–532

Hsu Y-J, Simons M, Yu S-B, Kuo L-C, Chen H-Y (2003) A two-dimensional dislocation model for interseismic deformation of the Taiwan mountaion belt. Earth Planet Sci Lett 211:287–294

Hsu Y-J, Segall P, Yu S-B, Kuo L-C, Williams C (2007) Temporal and spatial variations of postseismic deformation following the 1999 Chi-Chi, Taiwan earthquake. Geophys J Int 169:367–379. doi:10.1111/j.1365-246X.2006.03310.x

Hsu Y-J, Yu S-B, Simons M, Kuo L-C, Chen H-Y (2008) Interseismic crustal deformation in the Taiwan plate boundary zone revealed by GPS observations, seismicity, and earthquake focal mechanisms. Tectonophysics. doi:10.1016/j.tecto.2008.11.016

Huang CY, Cheng YM, Yeh CC (1985) Genesis of the Kenting Formation in the Hengchun Peninsula, southern Taiwan. Ti-Chih (Geology) 6:21–38

Huang C-Y, Yuan P, Tsao S-J (2006) Temporal and spatial records of active arc-continent collision in Taiwan: a synthesis. Geol Soc Am Bull 118(3/4):274–288. doi:10.1130/B25527.1

Huang CY, Chien C-W, Yao B, Chang CP (2008) The Lichi Melange: a collision melange formation along early arcward backthrusts during forearc basin closure, Taiwan arc-continent collision. In: Draunt AE, Clift PD, Scholl D (eds) Formation and applications of the sedimentary record in arc collision zones, vol 436. Geological Society of America, Boulder, pp 127–154

Hung JH, Wiltschko DV (1993) Structure and kinematics of arcute thrust faults in teh Miaoli-Cholan area of western Taiwan. Petrol Geol Taiwan 8:59–96

Jordon TE (1995) Retroarc Foreland and related basins. In: Busby C, Ingersoll R (eds) Tectonics of sedimentary basins. Blackwell, Oxford, pp 331–362

Khan M, Treloar P, Searle M, Jan M (eds) (2000) In: Tectonics of the Nanga Parbat Syntaxis and the Western Himalaya, vol 170. Geological Society of London, Special Publications, London. doi:10.1144/GSL.SP.2000.170.01.01

Kim K-H, Huang B, Yeh Y-H, Shen P, Chiu J-M, Pujol J, Chen K-C (2005) Three-dimensional Vp and Vs structural models associated with the active subduction and collision tectonics in the Taiwan region. Geophys J Int 162(1):204–220

Koons PO (1990) The two-sided orogen: collision and erosion from the sandbox to the Southern Alps, New Zealand. Geology 18:679–682

Lacombe O, Mouthereau F, Angelier J, Deffontaines B (2001) Structural, geodetic and seismological evidence for tectonic escape in sw Taiwan. Tectonophysics 333:323–345

Lacombe O, Mouthereau F, Angelier J, Chu H-T, Lee J-C (2003) Frontal belt curvature and oblique ramp development at an obliquely collided irregular margin: geometry and kinematics of the NW Taiwan fold-thrust belt. Tectonics 22 (3). doi:10.1029/2002TC001436

Lee Y-H, Byrne T, Lo W (2010) Exhumation History and Segmentation of the Hsuehshan Range, Central Taiwan Revealing by Low Temperature Thermochronology Data, American Geophysical Union: Taipei, AGU, p. T54A-01

Lee C-R, Cheng W-T (1986) Preliminary heat flow measurements in Taiwan. In: Proceedings of the fourth circum-pacific energy and mineral resources conference, Singapore

Lee T-Q, Kissel C, Barrier E, Laj C, Chi W-R (1991) Paleomagnetic evidence for a diachronic clockwise rotation of the Coastal Range, eastern Taiwan. Earth Planet Sci Lett 104: 245–257

Lee J-C, Lu C-Y, Chu H-T, Delcaillau B, Angelier J, Deffontaines B (1996) Active Deformation and Paleostress Analysis in the Pakua Anticline Area of Western Taiwan. Terr Atmos Ocean Sci 7(4):431–446

Lee J-C, Deffontaines B, Angelier J, Chu H-T, Hu J-C, Lacombe O, Mouthereau F, Yeh Y-H, Bureau D, Carvalho J, Lu C-Y, Liew P-M, Rudant J-P, Li F-C, Jeng J-C, Lee C-T (1997) Morphoneotectonic map of Taiwan. Central Geologic Survey, Ministry of Economic Affairs, R.O.C

Lee Y-H, Hsieh M-L, Lu S-D, Shih T-S, Wu W-Y, Sugiyama Y, Azuma T, Kariya Y (1999) Slip vectors of the surface rupture of the 1999 Chi-Chi earthquake, western Taiwan. J Struct Geol 25:1917–1931

Lee J-C, Angelier J, Chu H-T, Hu J-C, Jeng F-S (2001) Continuous monitoring of an active fault in a plate suture zone: a creepmeter study of the Chihshang Fault, eastern Taiwan. Tectonophysics 333:219–240

Lee J-C, Hu J-C, Rau RJ (2002) Near-surface seasonal creeping and subsurface repeated seismicity on the plate-suture thrust fault in Chihshang, Eastern Taiwan. Eos Trans AGU 83(47) FallMeet Suppl, Abstract T61B-1276

Lee Y-H, Chen C-C, Liu T-K, Ho H-C, Lu H-Y, Lo W (2006) Mountain building mechanisms in the Southern Central Range of the Taiwan Orogenic Belt – from accretionary wedge deformation to arc–continental collision. Earth Planet Sci Lett 252:413–422. doi:10.1016/j.epsl.2006.09.047

Lee C-P, Hirata N, Huang B, Huang W-G, Tsai Y-B (2009) Anomalous seismic attenuation along the plate collision boundary in southeastern Taiwan: observations from a linear seismic array. Bull Seismol Soc Am 99:2662–2680. doi:10.1785/0120080302

Lee C-P, Hirata N, Huang B-S, Huang W-G, Tsai Y-B (2010) Evidence of a highly attenuative aseismic zone in the active collision orogen of Taiwan. Tectonophysics 489:128–138. doi:10.1016/j.tecto.2010.04.009

Liew P-M, Pirazzoli PA, Hsieh M-L, Arnold M, Barusseau JP, Fountugne M, Giresse P (1993) Holocene tectonic uplift deduced from elevated shorelines, eastern Coastal Range of Taiwan. Tectonophysics 222:55–68

Lin C-H (2000) Thermal modeling of continental subduction and exhumation constrained by heat flow and seismicity in Taiwan. Tectonophysics 324:189–201

Lin CH, Roecker SW (1993) Deep earthquakes beneath central Taiwan: mantle shearing in an arc-continent collision. Tectonics 12(3):745–755

Lin AT-S, Watts A (2002) Origin of the west Taiwan basin by orogenic loading and flexure of a rifted continental margin. J Geophys Res 107(B9):2185. doi:10.1029/2001JB000669

Lin C-H, Yeh Y-H, Yen H-Y, Chen K-C, Huan B-S, Roecker SW, Chiu J-M (1998) Three-dimensional elastic wave structure of the Hualien region of Taiwan: evidence of active crustal exhumation. Tectonics 17:89–103

Lin A, Watts A, Hesselbo P (2003) Cenozoic stratigraphy and subsidence history of the South China Sea margin in the Taiwan region. Basin Res 15:453–478. doi:10.1046/j.1365-2117.2003.00215.x

Lin K-C, Hu J-C, Ching K-E, Angelier J, Rau R-J, Yu S-B, Tsai C-S, Shin T-C, Huang M-H (2010) GPS crustal deformation, strain rate and seismic activity after the 1999 Chi-Chi earthquake in Taiwan. J Geophys Res 115 (B07404) 22 pp

Liu CC, Yu SB (1990) Vertical crustal movements in eastern Taiwan and their tectonic implications. Tectonophysics 183:111–119

Liu T-K, Chen Y-G, Chen W-S, Jiang S-H (2000) Rates of cooling and denudation of the Early Penglai Orogeny, Taiwan, as assessed by fission-track constraints. Tectonophysics 320:69–82

Liu T-K, Hsieh S, Chen Y-G, Chen W-S (2001) Thermo-kinematic evolution of the Taiwan oblique-collision mountain belt as revealed by zircon fission track dating. Earth Planet Sci Lett 186:45–56

Lo C-H, Onstott TC (1995) Rejuvenation of K-Ar systems for minerals in the Taiwan Mountain Belt. Earth Planet Sci Lett 131:71–98

Lu C-Y, Malavieille J (1994) Oblique convergence, indentation and rotation tectonics in the Taiwan mountain belt. Earth Planet Sci Lett 121:93–108

Lu C-Y, Chan Y-C, Kuo L-C, Chang K, Lee J-C (2010) Geohazards in related to neotectonic patterns of taiwan based on recent multi-source data. Paper presented at the EOS Trans. AGU, Taipei, Taiwan

Lundberg N, Dorsey RJ (1990) Rapid Quaternary emergence, uplift, and denudation of the Coastal Range, eastern Taiwan. Geology 18:638–641

Macedo JM, Marshak S (1999) Controls on the geometry of fold-thrust belt salients. Geol Soc Am Bull 111:1808–1822

Malavieille J, Trullenque G (2009) Consequences of continental subduction on forearc basin and accretionary wedge deformation in SE Taiwan: insights from analogue modeling. Tectonophysics. doi:10.1016/j.tecto.2007.11.016

Marshak S (2004) Salients, recesses, arcs, orocline, and syntaxes – a review of ideas concerning the formation of map-view curves in fold-thrust belts. In: McClay KR (ed) Thrust tectonics and hydrocarbon systems, vol 82, AAPG Memoir. American Association of Petroleum Geologists, Tulsa, pp 131–156

McCabe R (1984) Implications of paleomagnetic data on the collision-related bending of island arcs. Tectonics 4: 409–428

McIntosh K, Nakamura Y, Wang T-K, Shih R-C, Chen A, Liu C-S (2005) Crustal-scale seismic profiles across Taiwan and the western Philippine Sea Plate. Tectonophysics 401: 23–54

Mouthereau F, Lacombe O (2006) Inversion of the Paleogene Chinese continental margin and thick-skinned deformation in the Western Foreland of Taiwan. J Struct Geol 28: 1977–1993.

Mouthereau F, Deffontaines B, Lacombe O, Angelier J (2002) Variations along the strike of the Taiwan thrust belt: basement control on the structural style, wedge geometry and kinematics. In: Byrne T, Liu C-S (eds) Geology and geophysics of an arc-continent collision, Taiwan, vol 358, Geologic Society of America Special Paper. Geologic Society of America, Boulder, CO

Namson J (1981) Detailed structural analysis of the western foothills belt in the Miaoli-Hsinchu area, Taiwan: I Southern Part. Petrol Geol Taiwan 18:31–51

Nissen S, Hayes DE, Bochu Y, Weijun Z, Yongqin C, Xiaupin N (1995) Gravity, heat flow, and seismic constraints on the processes of crustal extension: Northern margin of the South China Sea: Journal of Geophysical Research, v. 100, no. B11, p. 22,447–422,483

Nissen S, Hayes DE, Buhl P, Diebold J, Bochu Y, Weijun Z, Yongqin C (1995) Deep penetration seismic soundings across the northern margin of the South China Sea. J Geophys Res 100(B11):22407–22433

Page B, Lan CY (1983) The Kenting melange and it's tectonic events. Mem Geol Soc China 5:227–248

Page BM, Suppe J (1981) The Pliocene Lichi melange in Taiwan: its plate tectonic and olistostromal origin. Am J Sci 281:193–227

Perfettini H, Avouac J-P (2004) Postseismic relaxation driven by brittle creep: a possible mechanism to reconcile geodetic measurements and the decay rate of aftershocks, application to the Chi-Chi earthquake, Taiwan. J Geophys Res 109 (B02304). doi:10.1029/2003JB002488

Pulver MH, Crespi JM, Byrne TB (2002) Lateral extrusion in a transpressional collisional zone: an example from the pre-Tertiary metamorphic basement of Taiwan. In: Byrne TB, Liu C-S (eds) Geology and geophysics of an arc-continent collision, Taiwan, vol 358, Geological Society of America Special Paper., pp 107–120

Ramsay LA, Walker RT, Jackson J (2007) Geomorphic constraints on the active tectonics of southern Taiwan. Geophys J Int. doi:10.1111/j.1365-246X.2007.03444.x

Rau R-J, Wu F (1995) Tomographic imaging of lithospheric structures under Taiwan. Earth Planet Sci Lett 133:517–532

Rau R-J, Wu FT (1998) Active tectonics of Taiwan orogeny from focal mechanisms of small-to-moderate-sized earthquakes. Terr Atmos Ocean Sci 9:755–778

Roecker SW, Yeh YH, Tsai Y-B (1987) Three-dimensional P and S wave velocity structures beneath Taiwan deep structure beneath an arc continent collision. J Geophys Res 92: 10547–10570

Ryan WBF, et al. (2009) Global Multi-Resolution Topography synthesis, Geochem. Geophys. Geosyst., 10, Q03014, doi:10.1029/2008GC002332

Seno T, Stein S, Gripp AE (1993) A model for the motion of the Philippine Sea plate consistent with NUVEL-1 and geologic data. J Geophys Res 98:17941–17948

Shyu JH, Sieh K, Chen Y-G, Chung L-H (2006) Geomorphic analysis of the Central Range fault, the second major active structure of the Longitudinal Valley suture, eastern Taiwan. Geol Soc Am Bull 118(11/12):1447–1462. doi:10.1130/B25905.1

Simoes M, Avouac J-P (2006) Investigating the kinematics of mountain building in Taiwan from the spatiotemporal evolution of the foreland basin and western foothills. J Geophys Res 111. doi:10.1029/2005JB004209

Simoes M, Avouac J-P, Beyssac O, Goffe B, Farley K, Chen Y-G (2007) Mountain building in Taiwan: a thermokinematic model. Journal of Geophysical Research 112. doi:10,1029/2006JB004824

Stanley RS, Hill AB, Chang HC, Hu HN (1981) A transect through the metamorphic core of the Central Mountains, southern Taiwan. Memoirs Geol Soc China 4:443–473

Stolar D, Roe GH, Willett S (2007a) Controls on the patterns of topography and erosion rate in a critical orogen. J Geophys Res 112 (F04002)

Stolar D, Willett S, Montgomery DR (2007b) Characterizing topographic steady state in Taiwan. Earth Planet Sci Lett 261: 421–431

Suppe J (1981) Mechanics of mountain building and metamorphism in Taiwan. Memoir Geol Soc China 4:67–89

Suppe J (1984) Kinematics of arc-continent collision, flipping of subduction and back-arc spreading near Taiwan. Memoirs Geol Soc China 6:21–33

Suppe J, Wu YM, Carena S, Ustaszewski K (2010) Deep and shallow structure of the Taiwan arc-continent collision. In: West. Pac. Geophys. Meet. Suppl., Taipei, Taiwan. Eos Trans AGU. pp Abstract T22A-01

Teng LS (1987) Stratigraphic records of the late Cenozoic Penglai orogeny of Taiwan. Acta Geologica Taiwanica 25: 205–224

Teng LS (1990) Geotectonic evolution of late Cenozoic arc-continent collision in Taiwan. Tectonophysics 183:57–76

Teng LS (1996) Extensional collapse of the northern Taiwan mountain belt. Geology 24(10):949–952

Thomas W (2006) Tectonic inheritance at a continental margin. GSA Today 16(2):4–11

Tsan SF (1974) The Kenting formation: a note on Hengchun Peninsula stratigraphy. Proc Geol Soc China 17:131–133

Tsao S (1996) The geological significance of illite crystallinity, zircon fission-track ages and K-Ar ages of metasedimentary rocks of the Central Range. M.S., National Taiwan University, Taipei

Vogt PR, Lowrie A, Bracey D, Hey R (1976) Subduction of aseismic oceanic ridges: effects on shape, seismicity, and other characteristics of consuming plate boundaries. Geol Soc Am Spec Publ 172:59

Wallace L, McCaffery R, Beaven J, Ellis S (2005) Rapid microplate rotations and backarc rifting at the transition between collision and subduction. Geology 33(11):857–860

Wang C, Huang C-P, Ke L-Y, Chien W-J, Hsu S-K, Shyu C-T, Cheng W-B, Lee C-S, Teng LS (2002) Formation of the Taiwan Island as a solitary wave along the Eurasian continental plate margin: magnetic and seismological evidence. Terr Atmos Ocean Sci 13(3):339–354

Wang TK, Chen M-K, Lee C-S, Xia K (2006) Seismic imaging of the transitional crust across the northeastern margin of the South China Sea. Tectonophysics 412:237–254

Wang H-L, Chen H-W, Zhu L (2010a) Constraints on average Taiwan Reference Moho Discontinuity Model – receiver function analysis using BATS data. Geophys J Int 183: 1–19. doi:10.1111/j.1365-246X.2010.04692.x

Wang Y-J, Ma K-F, Mouthereau F, Eberhart-Phillips D (2010b) Three-dimensional Qp- and Qs-tomography beneath Taiwan orogenic belt: implications for tectonic and thermal structure. Geophys J Int 180(2):891–910. doi:10.1111/j.1365-246X.2009.04459

Whipple KX, Meade B (2004) Controls on the strength of coupling among climate, erosion, and deformation in two-sided, frictional orogenic wedges at steady state. J Geophys Res 109. doi:10.1029/2003JF000065

Whipple KX, Meade B (2006) Orogen response to changes in climatic and tectonic forcing. Earth Planet Sci Lett 243: 218–228. doi:10.1016/j.epsl.2005.12.022

Willemin J, Knuepfer P (1994) Kinematics of arc-continental collision in the eastern Central Range of Taiwan inferred from geomorphic analysis. J Geophys Res 99(B10):20, 267–20, 280

Willett S, Beaumont C, Fullsack P (1993) Mechanical model for the tectonics of doubly vergent compressional orogens. Geology 21(4):371–374

Willett S, Fisher DM, Fuller C, Yeh E-C, Lu C-Y (2003) Erosion rates and orgenic-wedge kinematics in Taiwan inferred from fission-track thermochronometry. Geology 31(11):945–948

Wiltschko D, Hassler L, Hung J-H, Liao H-S (2010) From Accretion to Collision: Motion and evolution of the Chaochou Fault, Southern Taiwan. Tectonics 29 (TC2015)

Wobus CW, Crosby BT, Whipple KX (2006) Hanging valleys in fluvial systems: controls on occurrence and implications for landscape evolution. J Geophys Res 111. doi:10.1029/2005JF000406

Wu FT, Rau RJ (1998) Seismotectonics and identification of potential seismic source zones in Taiwan. Terr Atmos Ocean Sci 9:739–754

Wu F, Rau R-J, Salzberg D (1997) Taiwan orogeny: thin-skinned or lithospheric collision? Tectonophysics 274:191–220

Wu FT, Chang LS, Wu YM (2004) Precisely relocated hypocenters, focal mechanism and active orogeny in central Taiwan. In: Malpas J, Fletcher CJ, Ali JR, Aitchison JC (eds) Aspects of the tectonic evolution of China, vol 226. Geological Society of London Special Publications, London, pp 333–354

Wu YM, Chang C-H, Zhao L, Shyu B, Chen Y-G, Sieh K, Avouac J-P (2007) Seismic tomography of Taiwan: improved constraints from a dense network of strong motion stations. J Geophys Res 112 (B08312). doi:10.1029/2007JB004983

Wu FT, Liang W, Lee J-C, Benz H, Villasenor A (2009) A model for the termination of the Ryukyu subduction zone against Taiwan: a junction of collision, subduction/separation, and subduction boundaries. Journal Geophysical Research 114 (B07404). doi:10.1029/2008JB005950

Yamato P, Mouthereau F, Burov E (2009) Taiwan mountain building: insights from 2-D thermomechanical modeling of a rheologically stratified lithosphere. Geophys J Int 176: 307–326. doi:10.1111/j.1365-246X.2008.03977

Yang TF, Tien JL, Chen C-H, Lee T, Punongbayan R (1995) Fission-track dating of the Taiwan-Luzon Arc: eruption ages and evidence for crustal contamination. J Asian Earth Sci 11:81–93

Yang T, Lee T, Chen C-H, Cheng S-N, Knittel U, Punongbayan R, Rasdas A (1996) A double island arc between Taiwan and Luzon: consequence of ridge subduction. Tectonophysics 258:85–101

Yang M, Rau R-J, Yu JC, Yu TT (2000) Geodetically observed surface displacements of the 1999 Chi-Chi, Taiwan, earthquake. Earth Planet Sci Lett 52:403–413

Yeh YH, Barrier E, Lin CH, Angelier J (1991) Stress tensor analysis in the Taiwan area from focal mechanisms of earthquakes. Tectonophysics 200:267–280

Yeh E-C, Fisher DM, Lu C-Y (2001) The structural evolution in the eastern central range of Taiwan. In: Program proceedings of the international symposium on East Asian Tectonics, Taipei, Taiwan, p 178

Yu H-S, Chou Y-W (2001) Characteristics and development of the flexural forebulge and basal unconformity of Western Taiwan Foreland Basin. Tectonophysics 333:277–291

Yu H-S, Huang Z-Y (2009) Morphotectonics and sedimentation in convergent margin basins: an example from juxtaposed marginal sea basin and foreland basin, Northern South China Sea. Tectonophysics 466:241–254. doi:10.1016/j.tecto.2007.11.007

Yu S-B, Cheng H-Y, Kuo L-C (1997) Velocity field of GPS stations in the Taiwan area. Tectonophysics 274:41–59

Yu S-B, Hsu Y-J, Kuo L-C, Chen H-Y, Liu C-C (2003) GPS measurement of postseismic deformation following the 1999 Chi-Chi, Taiwan, earthquake. J Geophys Res 108 (B11). doi:10.1029/2003JB002396

Yue L-F, Suppe J, Hung J-H (2005) Structural geology of a classic thrust belt earthquake: the 1999 Chi-Chi earthquake Taiwan (Mw = 7.6). J Struct Geol 27(11):2058–2083

Yui T-F, Wu TW, Jahn BM (1990) Geochemistry and plate-tectonic significance of the metabasites from the Tananao Schist Complex of Taiwan. J Southeast Asian Earth Sci 4:357–368